National sea level rise and coastal hazard analysis mapping for Vanuatu

April 2024

National sea level rise and coastal hazard analysis mapping for Vanuatu

A report submitted to the "Climate Information Services for Resilient Development in Vanuatu (VAN-CIS-RDP)" or *"Vanuatu Klaemaet Infomesen blong Redy, Adapt mo Protekt (Van-KIRAP)"*

April 2024

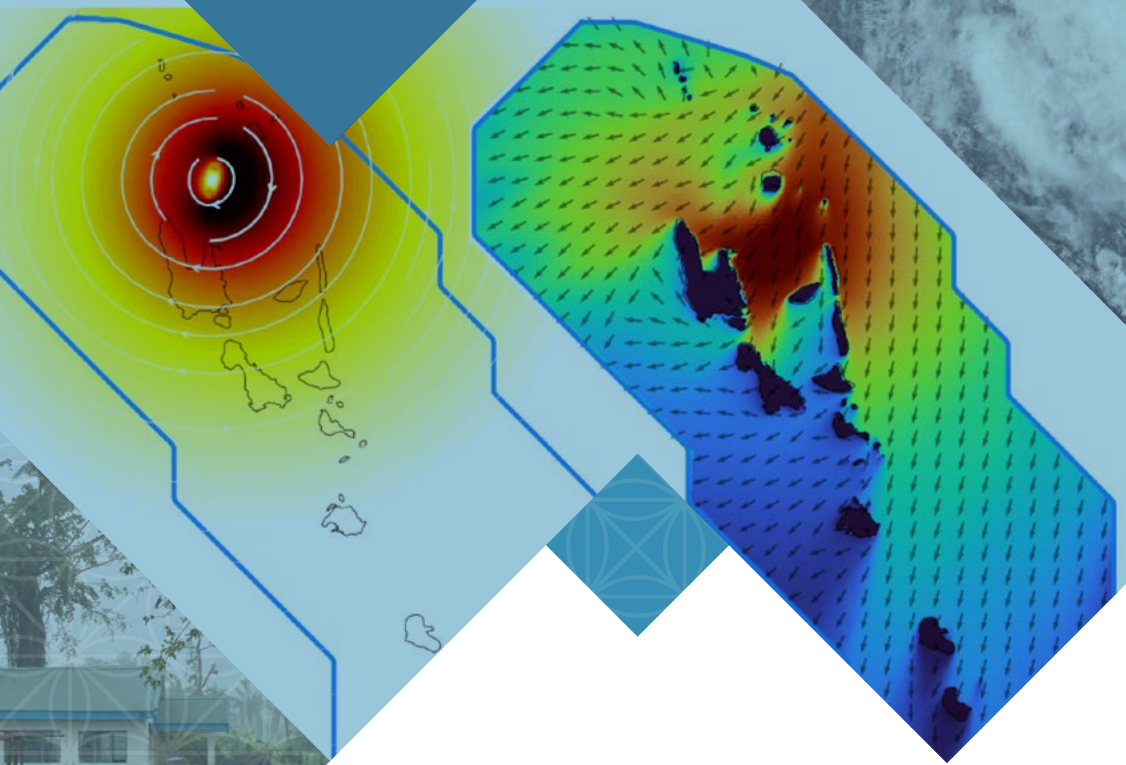

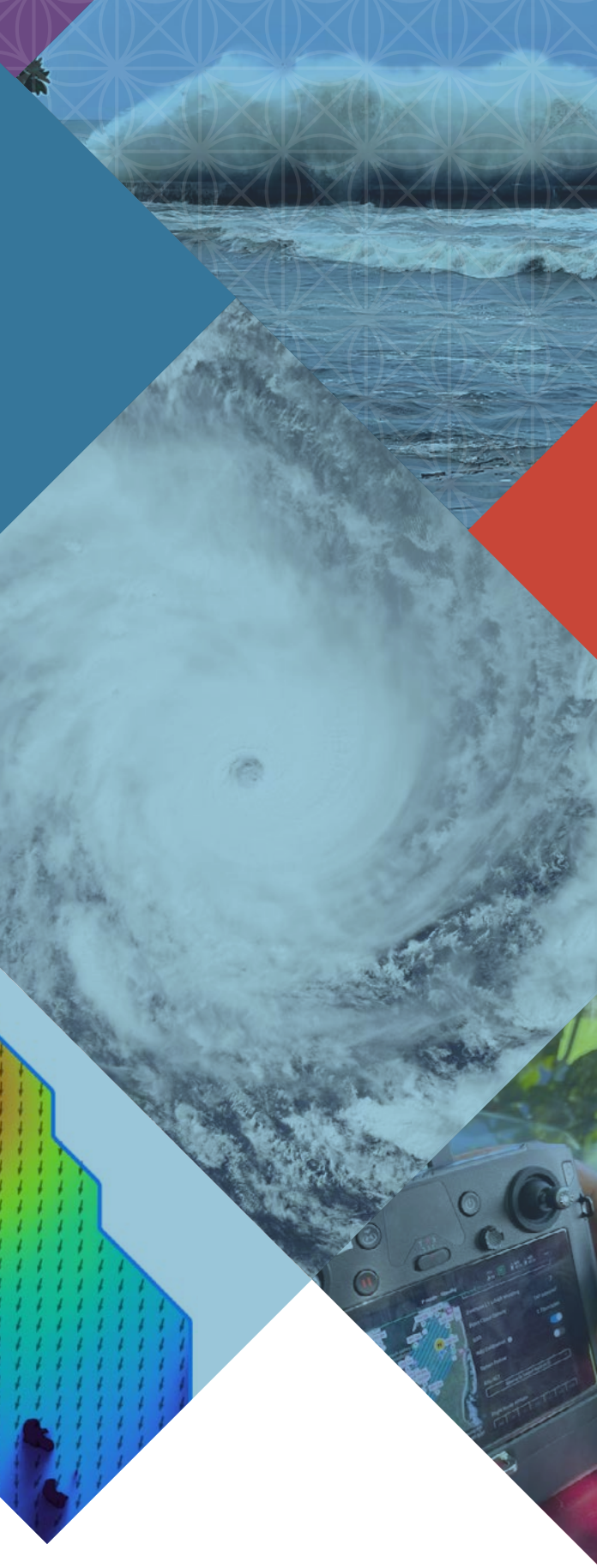

KLAEMET SAVE
REDI · ADAPT · PROTEKT

GREEN CLIMATE FUND

Citation

Hoeke RK, Hernaman V, van Vloten SO, Pérez-Díaz B, Ortiz-Angulo J, Echevarria E, Trenham C, Cagigal L, Hally B, Gregory R, Webb L, O'Grady J. (2023) National extreme sea level modelling and analysis under current and future sea level rise scenarios for Vanuatu. A report submitted to the "Climate Information Services for Resilient Development in Vanuatu (VAN-CIS-RDP)" or "*Vanuatu Klaemaet Infomesen blong Redy, Adapt mo Protekt (Van-KIRAP*)", CSIRO, Australia.

Copyright

Important disclaimer

Contents

Acknowledgments

Van-KIRAP Project is funded by the Green Climate Fund (GCF), implemented by the Secretariat of the Pacific Regional Environment Programme (SPREP) and executed jointly by SPREP and the Vanuatu Meteorological and Geo-hazards Department (VMGD) on behalf of the Government of Vanuatu. The Commonwealth Scientific and Industrial Research Organisation (Australia) is a designated Delivery Partner (DP) for the Van-KIRAP Project, and this report describes work completed by the CSIRO Climate Science Centre as specified in the Van KIRAP CSIRO DP Agreement and associated scope of work relating to Activity 1.2.4. Co-investment by CSIRO in this scope of work, as specified in the DP Agreement, is also acknowledged.

We thank all stakeholders, in particular SPREP, VMGD and those representing Van-KIRAP priority sectors (infrastructure, tourism, fisheries, agriculture and water) and associated sectors and interest groups and others who attended stakeholder engagements activities for this project.

We specifically acknowledge SPREP PMU including Van-KIRAP project managers and support staff, VMGD staff, Van KIRAP sector coordinators, other Van-KIRAP delivery partners and CSIRO project management and activity leads for their collaboration, coordination and inputs of knowledge and information.

We acknowledge the World Climate Research Programme's Working Group on Coupled Modelling, which is responsible for CMIP, and we thank the climate modelling groups for producing and making available their model output. For CMIP, the U.S. Department of Energy's Program for Climate Model Diagnosis and Intercomparison provides coordinated support and leads development of software infrastructure in partnership with the Global Organization for Earth System Science Portals.

Peer review (CSIRO): Kathleen McInnes and Geoff Gooley

Photo credits: Van-KIRAP Project

Executive summary

The report is developed by the Commonwealth Scientific and Industrial Research Organisation's Climate Science Centre (CSIRO CSC, Australia) for the *Climate Information Services for Resilient Development in Vanuatu (Van-KIRAP)* Project. Van-KIRAP is funded by the Green Climate Fund (GCF), implemented by the Secretariat of the Pacific Regional Environment Programme (SPREP) and delivered as joint execution entities by SPREP and the Vanuatu Meteorological and Geo-hazards Department (VMGD) on behalf of the Government of Vanuatu.

This report describes work completed by the CSIRO Climate Science Centre as specified in the Van-KIRAP CSIRO DP Agreement and associated scope of work relating to Activity 1.2.4. It is designed to assist VMGD with their effort toward outreach and communications of climate projections information in the form of Climate Information Services (CIS) to their sectoral and community-based stakeholders, including Van-KIRAP's targeted sectors (agriculture, fisheries, infrastructure, tourism and water). The report also serves as a technical reference and resource document for other users such as government officials, private sector, consultants, academia, NGOs, and donor agencies who have background knowledge about climate change and climate projections as relates to sea level rise, coastal inundation and associated hazards.

The key messages are summarised below.

- Future climate projections based on different greenhouse gas emissions scenarios suggest that sea-level rise (SLR) could range considerably by the end of the century, posing severe risks associated with inundation and erosion to the nation's low-lying coastal zones.
- Tropical cyclones (TCs) are the primary, but not the only, short-term driver of extreme sea level events which result in coastal inundation and coastal erosion.
- Existing tide gauge products and global or regional modelling outputs do not resolve these coastal hazards to adequately inform related local climate risk assessments and associated adaptation and mitigation strategies at the local community level.
- The national Van-KIRAP ocean-hazard modelling system described in this report has been developed to fundamentally improve nation-wide local estimation of coastal hazards at a finer spatial scale relevant to decision-making at local community level. This modelling system ability to simulate the dynamics of tides, storm surges, storm waves and background sea levels has been rigorously validated against tide gauges and satellite data.
- More specifically, the Van-KIRAP ocean-hazard modelling system has been used to simulate a 41-year historical hindcast as well as used as part of a probabilistic tropical cyclone (TC) assessment to gauge national extreme sea level scenarios under current sea level and future SLR conditions for Vanuatu.
- Extreme value analyses derived from this study have been utilized within Van-KIRAP's Climate Information Services (CIS) portal for risk-based mapping, enhancing Vanuatu's capabilities for science-based evidence to inform decision-making considering coastal and climate vulnerabilities and associated risks and adaptation planning.

- These new coastal hazard/climate products represent a significant step forward for Vanuatu's climate intelligence and associated CIS capabilities relevant over multi-decadal (current and future climate change) timescales. However, certain technical limitations in the methods and utility of the data must be acknowledged. These include model spatial resolution constraints, exclusion of certain dynamics (such as compound marine and fluvial/pluvial flooding) and exclusion of 'low likelihood high impact' SLR scenarios (associated with climate system tipping points). The report underscores the critical importance of integrating updated sea-level projections, new data and further local downscaling efforts in future work to better inform risk-based adaptation planning and decision-making, and thereby bolster national resilience against coastal impacts associated with climate change.

1 Introduction

1.1 Vanuatu – contextual setting

The Republic of Vanuatu is located in the South Pacific Ocean between latitudes 13 to 21°S and longitudes 166 to 171°E (Figure 1). Consisting of over 80 individual islands, the country was inhabited by over 307,000 people in 2022. The combination of the nation's exposure to natural hazards, extensive low-lying coastal zone, development stage and dependence on the natural-resources-based economy makes Vanuatu one of the most vulnerable nations to climate change in the world (The World Bank Group, 2021). Island nations such as Vanuatu are particularly vulnerable to increasingly frequent and severe flooding (inundation) and erosion impacts associated with global warming-induced sea level rise (SLR) (Nicholls et al., 2007; Seneviratne et al., 2012). As discussed in following sections, local exposure from inundation is highly modified by Tropical Cyclone (TC) activity and the El Niño Southern Oscillation (ENSO) variability, which provides important context for the work reported here.

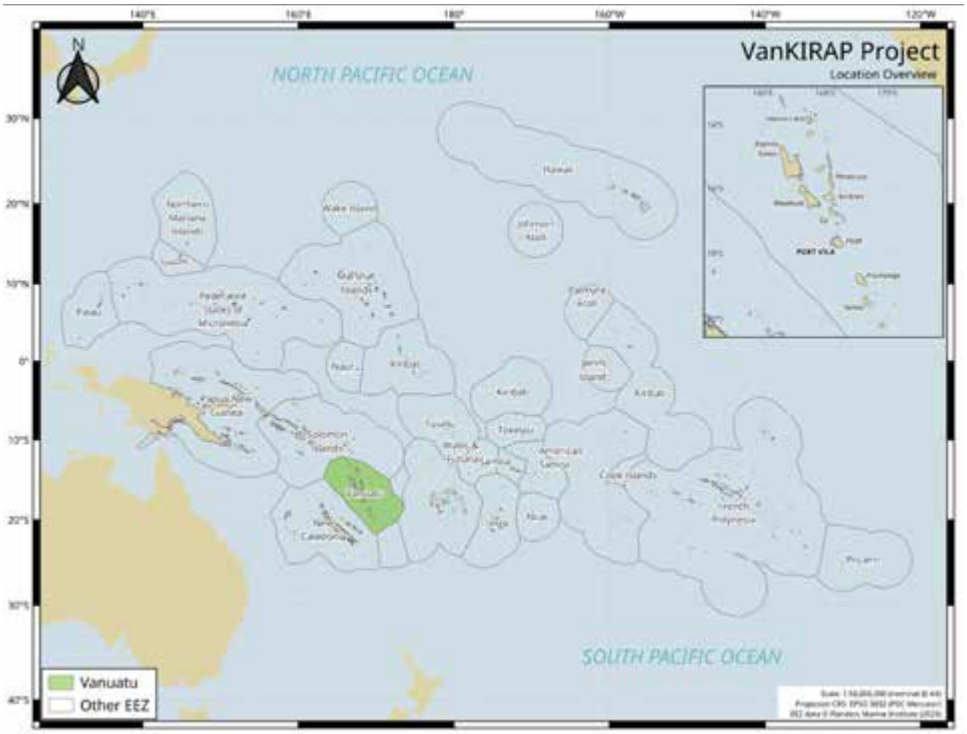

Figure 1: Overview of the location of Vanuatu within the Western Pacific Ocean.

1.2 Project background and the sea level rise/coastal hazard activity

Van-KIRAP's objectives are to build the technical capacity in Vanuatu to harness and manage climate data, in particular through development and delivery of practical Climate Information Services (CIS) tools and resources tailored to the needs of target sectors for informing adaptation planning, climate-based disaster risk management and associated decision-making. Additionally, the project is:

- facilitating enhanced coordination and dissemination of tailored CIS through purpose-built infrastructure such as the Vanuatu Climate Futures Portal, and the deployment of new coastal monitoring buoys for collection or real-time observational data, and
- supporting the application and demonstration of relevant CIS at sectoral level through real-time case studies.

These objectives are achieved through five of the project's Components:

- Component 1: Strengthen the VMGD platform to provide quality climate data and information for Climate Information Services (CIS)
- Component 2: Demonstrating the value of CIS at the sectoral and community levels
- Component 3: Development of CIS tools and engaging with stakeholders through outreach and communications
- Component 4: Strengthening the institutional capacity for long-term implementation of CIS in decision-making
- Component 5: Project coordination and management

One of the expected outputs of Component 1 is "Research, modelling and prediction to support CIS tools and uptake". Under this component, Activity 1.2.4 is tasked with:

Developing national-level current and future extreme sea level climatologies and associated CIS products for Vanuatu sector applications

This report describes the work undertaken and key findings including CIS products from Activity 1.2.4.

1.3 Background: sea level rise, extreme sea levels and coastal inundation hazards

1.3.1 Sea level rise

Overall long-term SLR is a global effect, however there are regional and even local differences. The observed SLR over the western tropical Pacific is about 10–15 cm on average between 1993 and 2020 (Marra et al., 2022), which is faster than in the central and eastern parts of the tropical Pacific (Fasullo & Nerem, 2018) (Figure 2). This has consequences for Vanuatu, particularly in low-lying coastal areas that are most vulnerable to flooding and erosion; in particular, immediately adjacent to local communities, natural resources, built assets and commerce/trade. Vertical land motion due to earthquakes, isostatic adjustment, compaction of sediments and other processes may influence local relative sea level (Brown et al., 2020) and can sometimes explain differences in long-term sea level trends between tide gauges and satellite altimetry. It should be noted that one of the main contributors to natural sea level variability on seasonal to interannual timescales is ENSO.

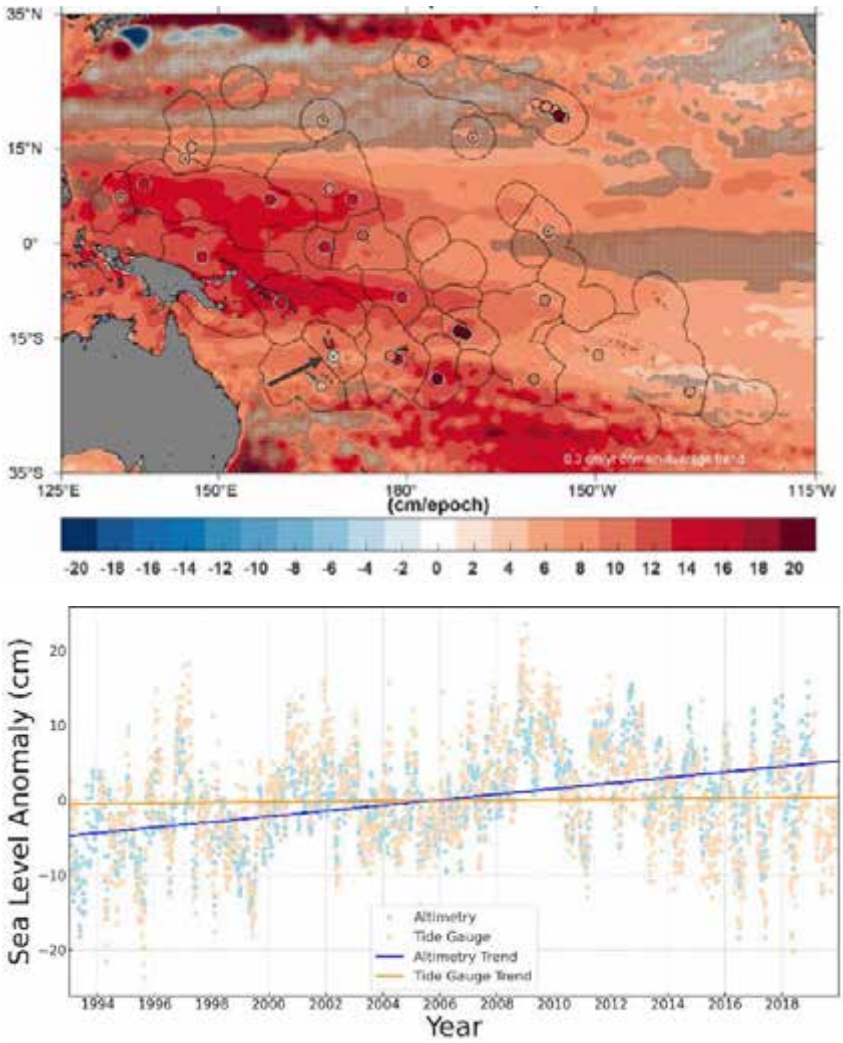

Figure 2: Top: Sea surface height (SSH) trends (cm/epoch) from satellite altimetry (shaded contours) and sea level trends from tide gauges (circles) during 1993–2020. Trends that are less than interannual variability, which is determined by the standard deviation of monthly anomalies, are indicated by hatching and circles with dots for the altimetry and tide gauges, respectively. An arrow points to Port Vila in Vanuatu. Source: [1] Bottom: SSH based on daily satellite altimeter data and relative sea level based on tide gauge data (see Sea Level Explorer Tool).

As discussed in section 1.1, future (projected) SLR is of particular concern to island nations; multiple lines of evidence indicate that global sea level will continue to increase well beyond the year 2100, regardless of which future greenhouse gas emissions (or concentration) scenario is adopted (Mengel et al., 2018). CMIP5 and CMIP6 climate models are incapable of simulating all the processes that contribute to SLR. In particular they do not account for ice sheet and glacier melt, which is a large component of current and projected SLR and the largest contributor to uncertainty in future sea levels. Separate cryosphere analyses are needed to account for these processes.

In the Van-KIRAP project we utilise data from the Pacific NextGen Projections for the Western Tropical Pacific: Current and Future Climate for Vanuatu (CSIRO & SPREP, 2021). The NextGen SLR projections for Vanuatu show a median rise of about 0.13 m by 2030 (Table 1) compared to a baseline of 1995 (1986–2005). By 2050, the rise is 0.23 m for low emissions (RCP2.6) and 0.28 m for high emissions (RCP8.5; also see Appendix D). By 2090, the rise is 0.42 m for low emissions and 0.73 m for high emissions (Table 1 and Figure 3).

Table 1 Median sea-level projections for Vanuatu with 5–95% uncertainty range relative to 1986–2005 for RCPs 2.6, 4.5, and 8.5. Units are metres. Source: (CSIRO & SPREP, 2021).

	RCP2.6		RCP4.5		RCP8.5	
2030	0.13	[0.10–0.17]	0.13	[0.09–0.17]	0.14	[0.10–0.18]
2050	0.23	[0.17–0.30]	0.24	[0.18–0.31]	0.28	[0.22–0.37]
2070	0.32	[0.24–0.43]	0.37	[0.28–0.48]	0.48	[0.37–0.64]
2090	0.42	[0.30–0.56]	0.50	[0.38–0.68]	0.73	[0.56–0.99]

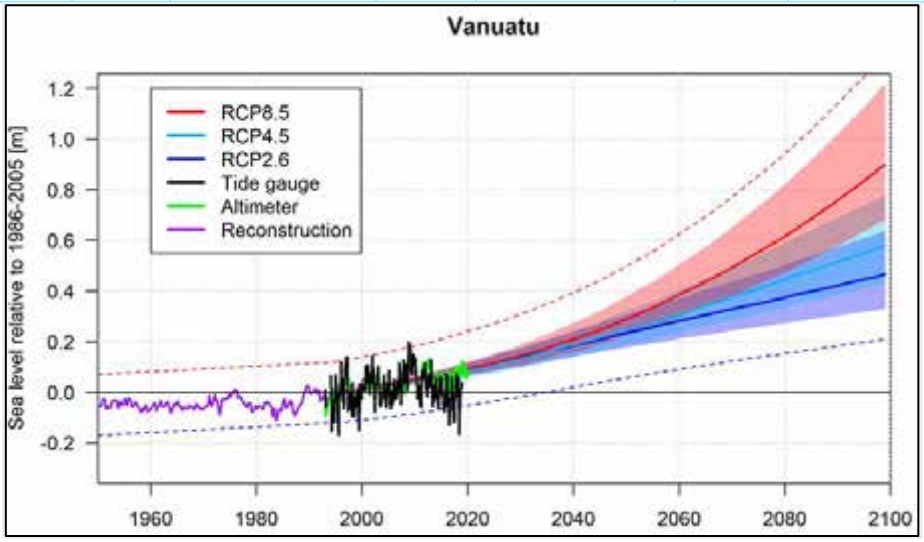

Figure 3: Time series of past and future sea level rise. Port Vila tide gauge records of relative sea level are indicated in black, the satellite record in green, reconstructed sea level data is shown in purple; all are monthly means and referenced to mean sea level between 1986-2005. Multi-model mean projections from 1995–2100 are given for three RCPs with the 5–95% uncertainty range shown by the shaded regions. The dashed lines are an estimate of month-to-month variability in sea level (5–95% uncertainty range about the projections and reconstruction) and indicate that individual monthly averages of sea level can be above or below longer-term averages.

1.3.2 Extreme sea level and coastal inundation

The previous section describes long-term trends in sea level for Vanuatu associated with climate change at a regional (western tropical Pacific) scale. At a finer spatial scale, any given coastal location's risk of being inundated at any given time is however due to a combination of factors, including tides, storm surges, storm waves and interannual sea level variability (due to climate variability such as ENSO; Figure 4). Local geomorphology influences the relative contributions of these different factors and how they combine to create extreme sea levels. For example, coastal bathymetry (shape of the seabed), especially the presence of offshore reefs, influence storm surges and wave-driven contributions. Offshore reefs cause waves to break offshore and thereby reduce the wave energy (and height) of the waves that eventually reach the coast. Steep shorelines (both with and without reefs) and greater offshore depths allow higher storm waves to reach the coast but are also less prone to the wind-driven components of storm surge (Figure 4).

The different contributions of tides, storm surge, storm waves and interannual sea level variability, and how they can combine to produce extreme sea levels, can be seen in observed total water level observations at Luganville and Port Vila (Figure 5a and 5c). These hourly water levels have been processed to separate tides due to the Sun and Moon (astronomical tides) from short-term non-tidal fluctuations (from storm surge and storm waves) and long-term changes (due to sea

level variability and rise). Extreme sea levels are rare and do not always occur due to a tropical cyclone; for instance, if a storm surge happens at low tide, the total water level may not be extreme at the adjacent coastline.

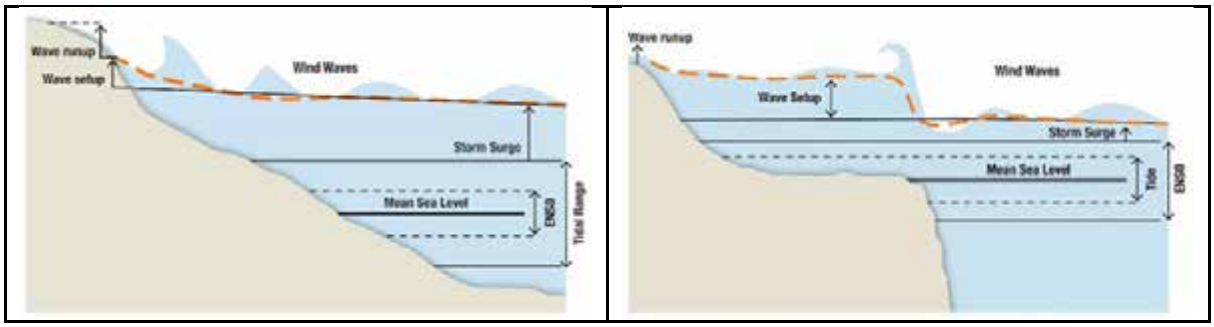

Figure 4: Schematic of the contributions of extreme sea levels at the coast for (a) a typical continental coastline and (b) for a reef fronted island.

Extreme value analysis (EVA) is a statistical method used to assess and characterize extreme events that have a low probability of occurring but can have significant consequences. These include impacts on critical infrastructure, amenity of local communities, commerce/trade and environmental resources such as protective shorelines, seagrass beds, mangroves, inshore reef structure etc. The average return period (also known as the average recurrence interval, ARI) is an EVA measure used to describe the average time between occurrences of an event of a certain magnitude (typically associated with known/expected impacts). It helps in quantifying the likelihood of an event happening within a given time frame. For example, a 50-year return period flood means, on average, a flood of that magnitude is expected to occur, on average, once every 50 years.

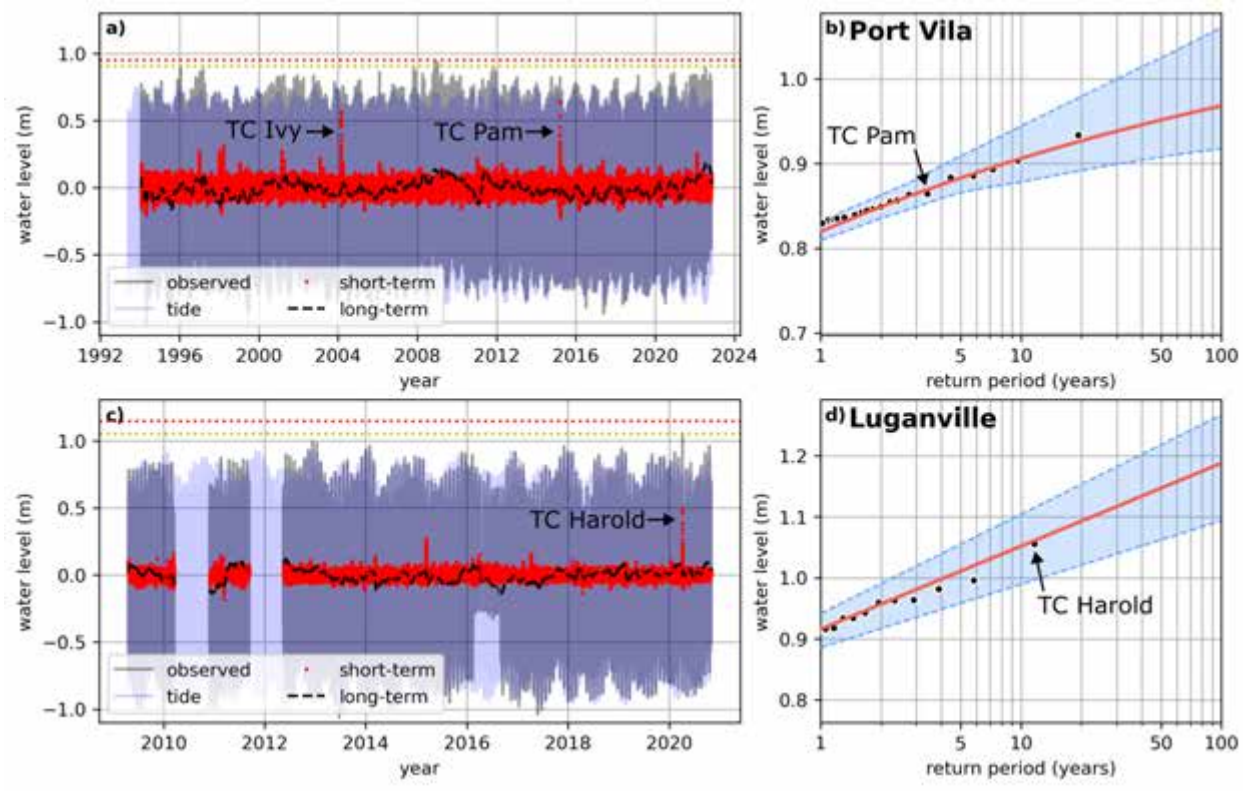

Figure 5: (a) hourly water levels from the Port Vila Tide Gauge; (b) extreme value analysis return periods based on the Port Vila Tide Gauge water levels; (c) hourly water levels from the Luganville Tide Gauge; (d) return periods

based on the Luganville Tide Gauge water levels. In subplots a and c, the 10-year and 50-year return intervals are indicated with horizontal yellow and red dotted lines respectively. In subplots b and d, the black dots represent the "empirical" return periods; the red lines and blue bands are the statistical fit and associated uncertainty (95% confidence limits) of the return periods.

Figure 5b and 5d show the return period curve resulting from the EVA applied to the observed extreme water levels at the Port Vila and Luganville tide gauges respectively. In this figure, the black dots represent the 'empirical' return periods at the tide gauges, the red lines are the statistical (generalised Pareto distribution fitted) return period prediction and the blue area represent the uncertainty of the prediction. Figure 5a and 5b show that although TC Pam had the highest (short term) storm surge sea level on record, it was not the highest observed total water level; that occurred in 2008 and was a combination of a very high spring tide and a high interannual (or long-term) sea level. Such natural events are sometimes called 'King Tides'.

While tide gauge observations and associated return periods for extreme sea levels can be valuable for hazard-based risk assessment and adaptation planning purposes, tide gauges are usually located in very sheltered harbours and extreme sea levels they observe are typically relevant only in the immediate area around the harbour. Pacific islands like Vanuatu tend to have high relative exposure to storm wave setup and runup, which is highly locally variable (Hoeke et al., 2021; Kennedy et al., 2012). Severe inundation may therefore occur in exposed areas, while tide gauges a short distance away (including on the same island) do not record particularly extreme sea levels (Hoeke et al., 2013; Wandres et al., 2020). The storm surge from TC Pam measured at the Port Vila Tide Gauge is an example of this: the total water level recorded at the tide gauge was minor compared to the catastrophic inundation and erosion that occurred a few kilometres along the east coast of Efate Island (Damlamian et al., 2017). An indication of the severity of the coastal impact can be found using the CAWCR Wave Hindcast (Durrant et al., 2014; Smith et al., 2020); it shows that wave heights off the south-east coast of Efate were by far the largest in the hindcast's entire 40+ year record (Figure 6). The EVA return periods for the CAWCR wave heights near Luganville and Port Vila also show something else: that extreme storm waves associated with cyclones occur only a few times during the 40+ year record; wave heights during TC Pam are so much higher than any other event in the hindcast record that it falls outside the confidence limits of the EVA imposed by the rest of the data. This relative rarity of extremes in the historical record translates into very high uncertainty in estimated EVA return periods (indicated in blue bands in Figure 6b and 6d). For instance, the uncertainty in the 100-year return wave height is between ~5 and ~12 m.

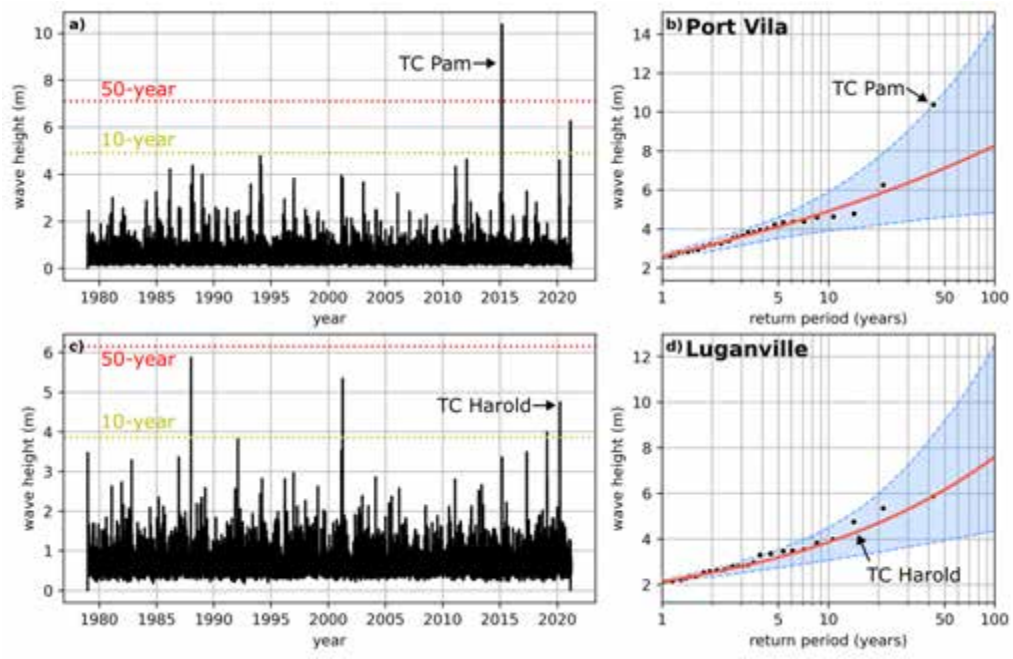

Figure 6: Hourly (significant) wave heights from the CAWCR Wave Hindcast and associated extreme value analysis return periods. Hourly wave heights (a) and return periods (b) for a point just offshore from the Port Vila Tide Gauge Location (near Pango Point); hourly wave heights (c) and return periods (d) for a point just offshore from the Luganville Tide Gauge location (east of Million Dollar Point). In subplots a and c, the 10-year and 50-year return intervals are indicated with horizontal yellow and red dotted lines respectively. In subplots b and d, the black dots represent the "empirical" return periods; the red lines and blue bands are the statistical fit and associated uncertainty (95% confidence limits) of the return periods.

In summary, the small number of long-term tide gauges with sufficiently reliable quality-controlled data to inform this study (currently only two: Port Vila and Luganville) and tide gauges' inability more generally to predict extreme sea levels just a short distance away means most locations in Vanuatu cannot rely on tide gauges alone to provide adequate coastal inundation risk information. While historical numerical reanalyses and hindcasts (like the CAWCR Hindcast) can provide more information, their spatial resolution is too coarse to resolve local exposure. Furthermore, EVA analysis of the relatively rare historically extreme TC-related storm wave and storm surge contributions to extreme sea levels results in highly uncertain estimates at the widely accepted probability horizons of (e.g.) 50- and 100-year return periods. Addressing these key uncertainties and delivering fundamentally improved national-scale coastal hazard (and ultimately coastal risk) information under both current and future sea level rise scenarios is a key component of this study for Van-KIRAP, as described in the next section.

To address the insufficient spatial resolution of relevant processes and local exposures, a national-scale numerical ocean hazard modelling system has been built for Vanuatu as part of this study, which is described in Section 2. This national system is then used to simulate a 41-year hindcast to provide verification of historical events and for EVA, described in Section 3. A suite of hybrid, probabilistic simulations is then used to better understand local exposure to relatively rare high-impact TCs and drastically reduce associated EVA uncertainties, particularly for lower probability/higher return period extreme sea level events. This is described in Section 4. Both the historic "mode" and probabilistic "mode" EVAs are combined with future projections of extreme sea levels for Vanuatu.

2 National Van-KIRAP ocean-hazard modelling system: description

The SCHISM-WWM3 coastal ocean model was selected to underpin the Van-KIRAP national ocean-hazard modelling system. SCHISM-WWM3 is a state-of-the-art numerical ocean modelling system widely used by the scientific community and industry for a range of regional and coastal scale applications (Zhang et al., 2016). The system is composed of a hydrodynamic circulation model and a wind-wave model that are two-way coupled (pass critical information to each other as the models perform their simulations) so they can account for non-linear current-wave interactions in the dynamic nearshore coastal zone. There are several other advantages in using SCHISM-WWM3:

- It runs on an unstructured mesh made up of triangular elements, which means it is very good at accurately representing complex coastlines and channels.
- High mesh resolution (small elements) can be easily placed in areas of complex bathymetry, to enable the model to accurately resolve local processes, which is much more difficult using structured (rectilinear or curvilinear) ocean models that often require nesting multiple model domains to achieve the required resolution transition.
- SCHISM-WWM3 is widely used by the international scientific community and industry. It is the model of choice for operational forecast systems in many countries (e.g., Central Weather Bureau of Taiwan; California Dept. of Water Resource; National Laboratory of Civil Engineering, Portugal) meaning it has been well tested and proven to be very reliable and accurate.

A key requirement for skilful coastal model simulations is accurate and high-resolution bathymetry. Obtaining realistic simulations of coastal ocean and nearshore processes using a numerical modelling approach is highly reliant on using accurate bathymetric data at sufficiently high resolution. Although global bathymetry data sets are available (e.g. GEBCO), these are not high enough resolution to meet project modelling requirements. As part of this activity, revised EOMAP (http://www.eomap.com/) satellite-derived bathymetry (Figure 7) was acquired and merged with PACCSAP-funded Vanuatu LiDAR data (https://www.pacificclimatechange.net/sites/default/files/LiDAR-Vanuatu) as well as other topographic and bathymetric data sources. The digital elevation models (DEMs) developed through this sub-activity are critically important to obtaining the realistic coastal extreme sea level and inundation simulations described in the next two sections. Furthermore, these DEM data sets will be of value to other sectoral applications, particularly fisheries, tourism, as well as representing an important resource for Vanuatu government agencies.

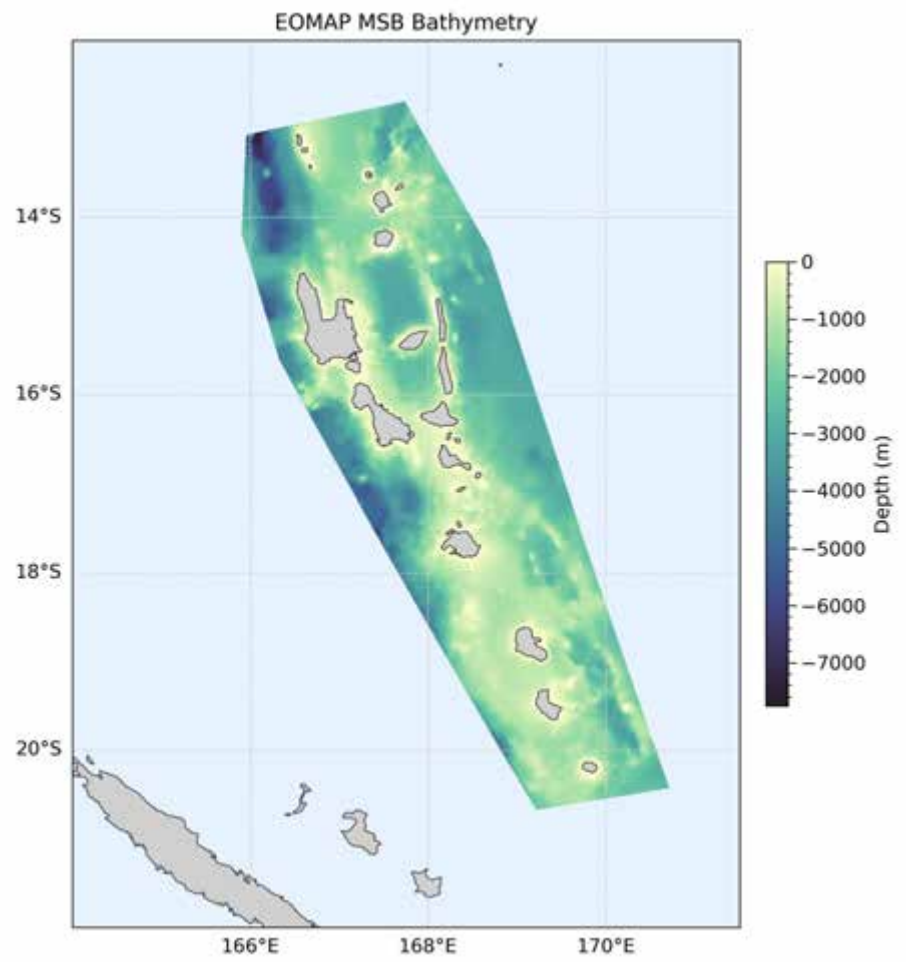

Figure 7: High-resolution satellite-derived bathymetry using revised EOMAP data, available for the entire Vanuatu archipelago.

The unstructured mesh developed for the Van-KIRAP national ocean-hazard modelling system contains approximately 110,000 computational nodes and 200,000 elements which vary from approximately 5 km near the lateral ocean boundaries and in deep (>>100 m) areas of the domain and reduce to approximately 100 m resolution near the shoreline where topographic and/or bathymetric LiDAR data is available and between 250 and 500 m resolution in other areas (this is shown in Figure 8). In addition to developing the computational mesh, the Allen Coral Atlas (https://allencoralatlas.org/) was used in combination with DEMs to discriminate between different seabed habitats and topographies within the computational mesh, so as to assign different hydraulic bed roughness coefficients. These are described in Section 3.1.

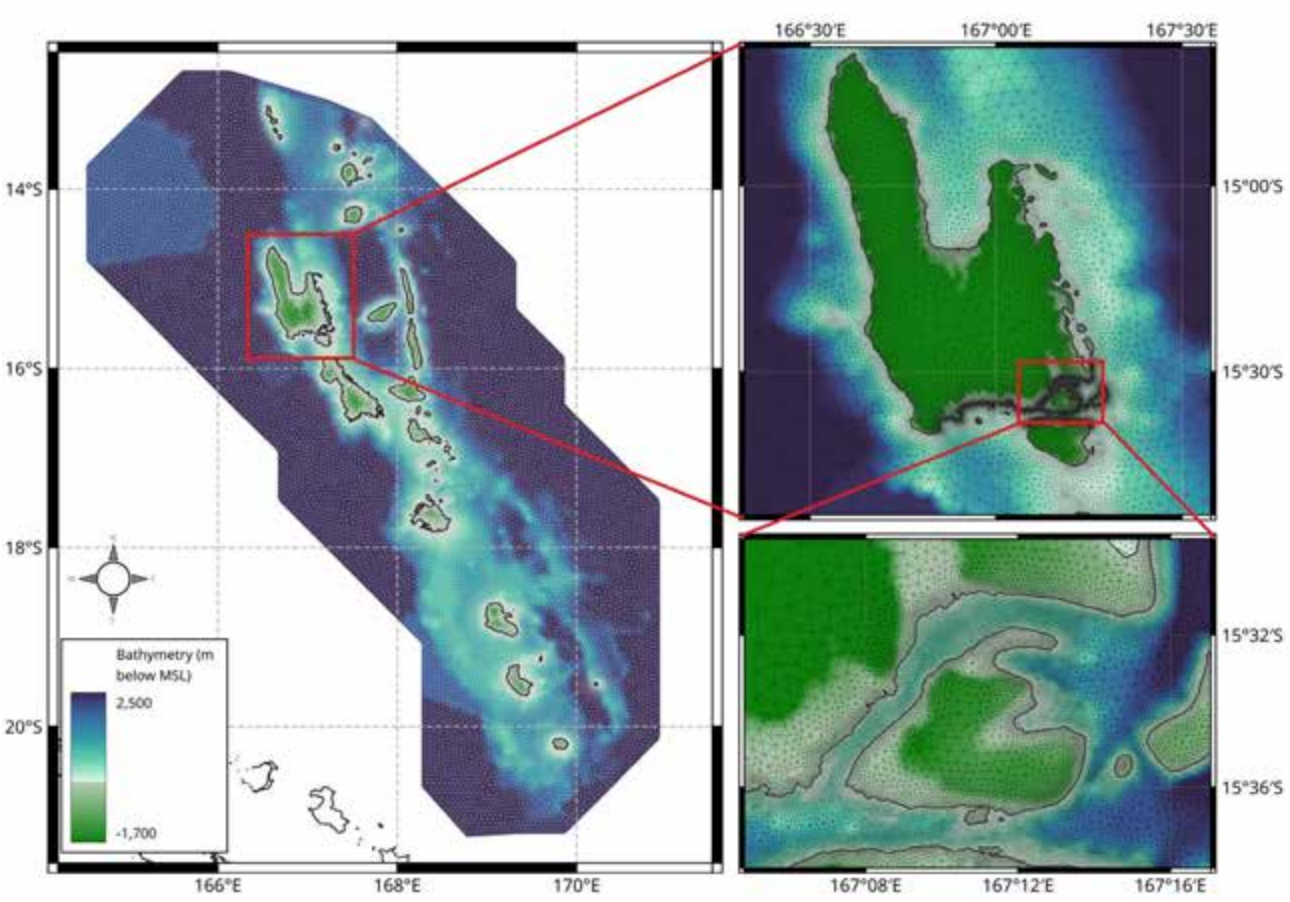

Figure 8: Domain for unstructured mesh model (left) and examples of the mesh at higher resolution showing seamless transitions between resolutions (right).

3 Ocean-hazard modelling system: verification and 41-year historical hindcast

A 41-year hourly historical hindcast (1980-2020) was generated based on the ocean-hazard SCHISM-WWM3 modelling system described in the previous section. This hindcast simulates the combined effects of tides, storm surge, waves, background sea level variability and rise for the entire period. The boundary conditions and atmospheric forcings developed are detailed below. Table 2 summarises the main information.

Table 2: Boundary conditions and forcing datasets used in the National Van-KIRAP ocean-hazard modelling system hindcast.

Astronomical tides and currents	TPXO version 9-atlas
Surface winds and sea-level pressure	NOAA CFSR
Sea level variability and rise	ECMWF ORAS5 (w/ geodetic correction)
Wind-waves	CAWCR Wave hindcast spectral output

Boundary Conditions:

- **Astronomical tide level and currents**. These components are specified by indicating the amplitudes and phases of the tidal constituents. This information is obtained from the TPXO global model of barotropic tide, obtained with methods described in detail by Egbert et al., (2002). These methods were implemented in the software package OTIS (OSU Tidal Inversion Software, https://www.tpxo.net). Specifically, the product used is the TPX09-atlas, a fully global solution obtained by combining 1/6-degree global solution TPXO9.v1 and thirty 1/30-degree resolution local solutions for all coastal areas.
- **Background sea level variability and vertical datum.** This time and space-varying ocean level component defined at the boundary nodes is obtained from ORAS5 global ocean reanalysis monthly data (https://cds.climate.copernicus.eu/cdsapp#!/dataset/reanalysis-oras5). This reanalysis combines model data with observations from across the world into a globally complete and dynamically consistent ocean dataset. ORAS5 has a temporal coverage from 1958 to present and a horizontal resolution of 0.25° x 0.25°. It is worth mentioning that the variable used, sea surface height, is the vertical distance between the actual sea surface and a reference surface of constant geopotential (geoid) with which mean sea level would coincide if the ocean were at rest. The geoidal heights of the input ORAS5 sea surface height is reduced to mean sea level (MSL) of the region by finding the mean sea level of the Noumea and Port Vila tide gauges for years 1990-1996 (a period of relatively low ENSO variability). This vertical reference datum of MSL between 1990-1996 is propagated throughout all total waver level (TWL) products delivered in this project.
- **Waves**. The hourly wave spectral information at the boundary is generated from the CAWCR wave hindcast (https://data.csiro.au/collection/csiro:39819). The CAWCR dataset is updated monthly from 1980 to present. It uses the WaveWatch III wave model forced with NCEP CFSR hourly winds and daily sea ice. The dataset contains spectral wave output

at 3683 points, as well as gridded outputs on a global 0.4-degree (24 arcminute) grid, with nested Australian and western Pacific sub-grids of 10 and 4 arcminutes resolution. For further information, see Durrant et al., (2014).

Atmospheric Forcings:

- **Wind and Pressure**. To be consistent with the forcing database of the CAWCR hindcast, the atmospherics fields of both are generated from NCEP CFSR (1980-2010, https://rda.ucar.edu/datasets/ds093.1/) and NCEP CFSRv2 (2011 to present, https://rda.ucar.edu/datasets/ds094.1/) hourly data.

The complete hindcast has been simulated on Australia-based high-performance computing (HPC) systems (NCI's Gadi, https://nci.org.au/). Annual simulations have been carried out, considering a 13-month year for each simulation and taking the first month as spin-up. The simulations have been run concurrently taking approximately 32 hours per simulation (192 CPUs and memory of 180 GB). The outputs are stored in monthly packages, containing hourly information on the whole mesh of the following key variables:

- zos – sea surface height above mean sea level (m);
- hs - significant wave height (m);
- t01 – mean wave period (sec);
- t02 – zero crossing mean wave period (sec);
- tp – peak wave period (sec);
- dp – peak wave direction (degrees North);
- spr – peak directional spreading (degrees);
- dp_rad – peak wave direction (radians); and
- u0, v0 – depth averaged velocity (lon and lat components) (ms^{-1}).

Outputs from the SCHISM-WWM3 model are supplied in NETCDF format, and are fully compliant with ACDD-1.3, CF-1.8 and UGRID-1.0 metadata conventions for climate-related data products. Optimisations have been applied to the raw SCHISM-WWM3 output to ensure easy display of information in geographic visualisation and processing packages such as QGIS.

3.1 Hindcast verification

Prior to running the entire hindcast several tuning periods and sensitivity tests were performed. Key tuning parameters included spatially varying Mannings and Madsen coefficients for circulation and wave-dependent bottom stress (Madsen et al., 1988), respectively. Table 3 shows the coefficients for different seabed types (as aggregated from the Allen Coral Atlas), which appear to optimise model skill when compared to the Port Vila and Luganville tide gauges as well as wave data from satellites and the Van-KIRAP Ocean Buoys, following sensitivity testing.

Like other researchers (e.g. Chen et al., 2019) we found it necessary to cap wind drag parameterisations to avoid unrealistically high wave heights under extreme TC conditions (Powell et al., 2003), i.e. winds greater than 50 m/s. The parameterisation described in this section are the most salient and are used for all subsequent simulations described in this report, including the synthetic TC simulations described in Section 4.

Table 3: Mannings and Madsen bottom stress coefficients selected for use in the Van-KIRAP national ocean-hazard modelling system.

Bed type	Mannings	Madsen
Ocean	0.02	0.03
Shallow bays/non-reef shoreline	0.03	0.03
Reefs	0.06	0.03
Land	0.17	N/A

Following these tuning steps, the overall hindcast performance verification, based on *in situ* observations (from tide gauges and new Spotter wave buoys), as well as satellite altimetry-derived wave information was performed. Overall comparisons of *in situ* observations to model hindcast output are listed in Table 4. The following subsections discuss these verification data sets and comparison to the hindcast in more detail.

Table 4: Root-mean-square error (RMSE), bias and Pearson correlation coefficient (R) for the key simulation variables water level and significant wave height, at long-term tide gauge stations and Spotter wave buoys.

Variable	Observation type	RMSE (m)	Bias (m)	R
water level	Luganville Tide Gauge	0.086	-0.025	0.981
	Port Vila Tide Gauge	0.083	-0.016	0.976
wave height	Luganville Spotter Buoy	0.101	0.016	0.825
	Port Vila Spotter Buoy	0.108	0.001	0.427

3.1.1 Tide gauges

Long-term tide gauge (TG) observations are available at Port Vila (from 1993 to 2021) and at Luganville (from 2008 to 2021). Hourly records for these time periods were provided by the Australian Bureau of Meteorology (http://www.bom.gov) and/or the Hawaii Sea Level Center (https://uhslc.soest.hawaii.edu/) and were used to validate the Vanuatu hindcast. While Table 4 presents comparison statistics for the entire available time periods of TG observations, Figures 9 and 10 show the respective comparison with Port Vila and Luganville TGs during the time of TC Harold. Figure 11 shows quantile-quantile (QQ) plots for the entire period and illustrates the excellent agreement between TG measured water levels and those simulated by the Van-KIRAP national ocean-hazard modelling system, including the extreme sea levels associated with TCs.

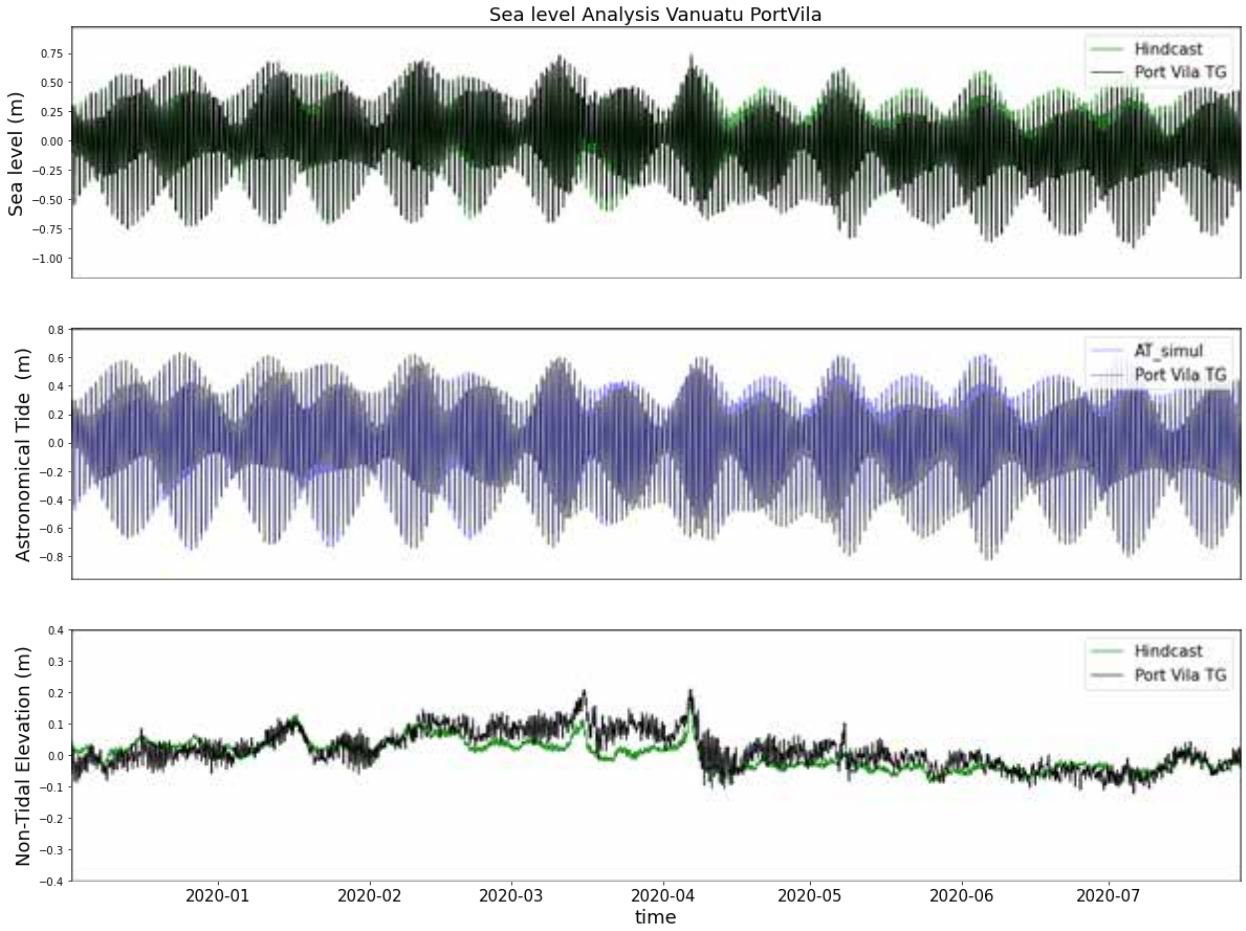

Figure 9: Comparison between the levels obtained from the hindcast and the Port Vila tide gauge records for the time of TC Harold.

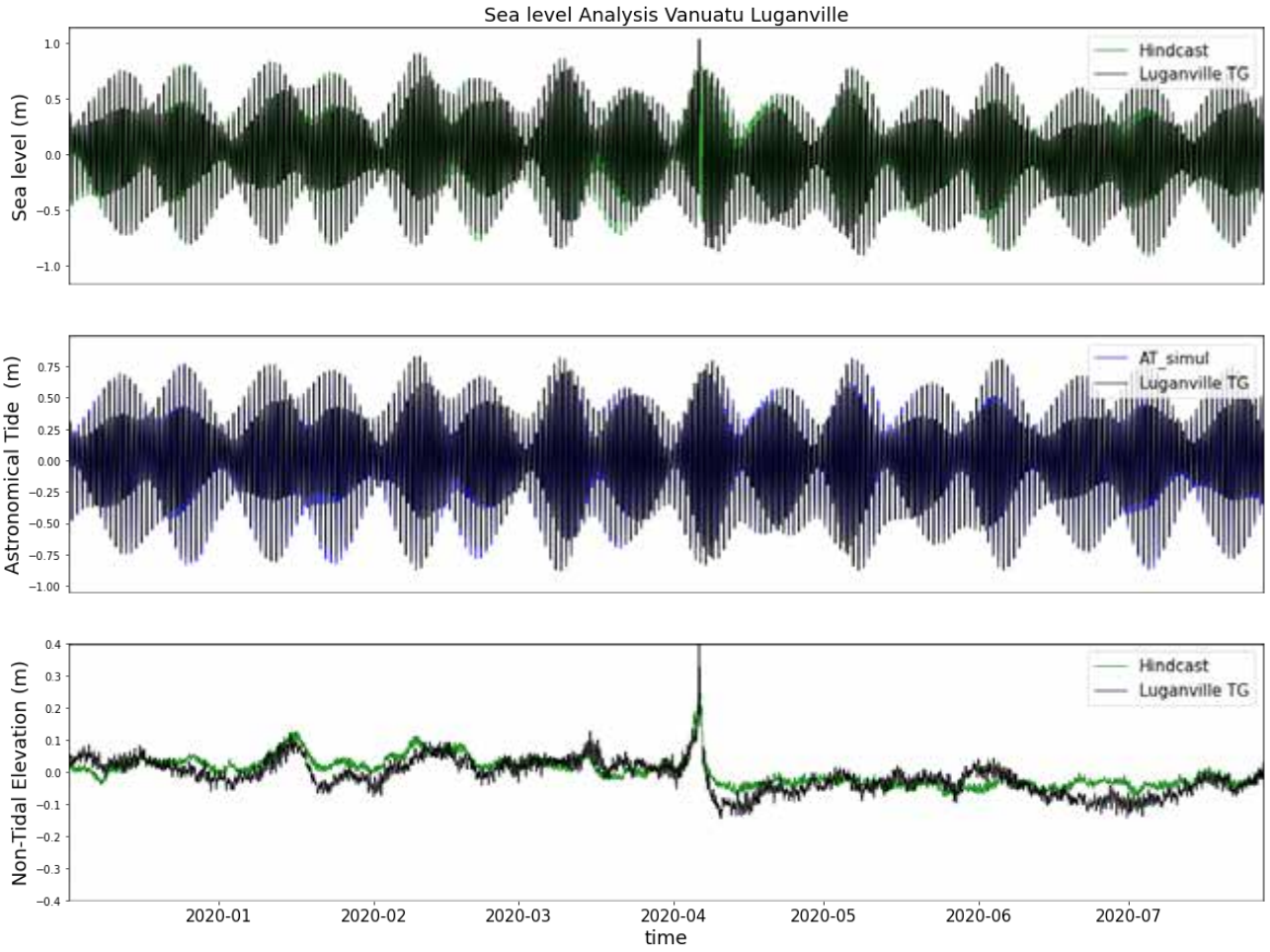

Figure 10: Comparison between the levels obtained from the hindcast and the Luganville tide gauge records for the time of TC Harold.

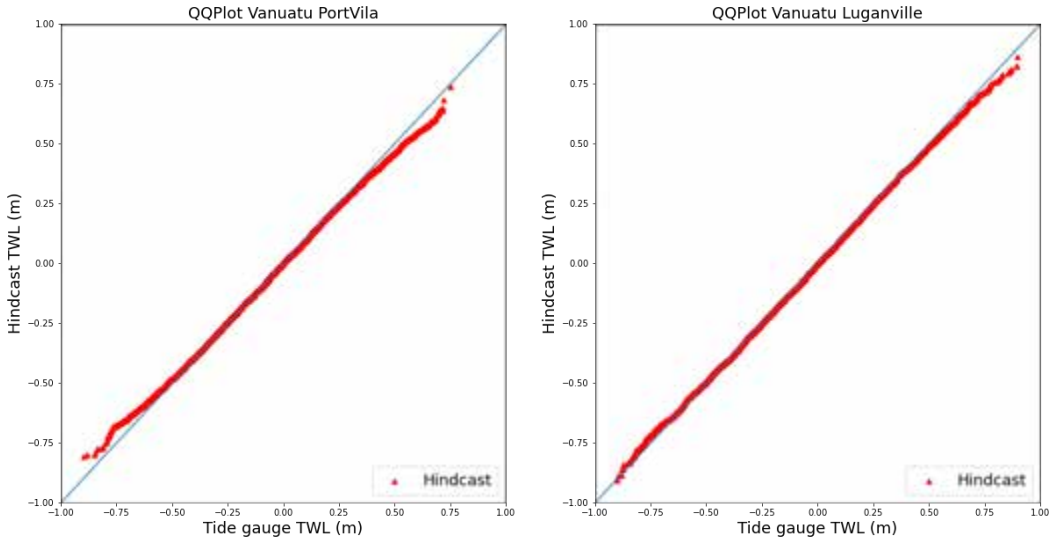

Figure 11: QQ-Plot comparisons between total water level (TWL) simulated by the hindcast and from tide gauge measurements for (left) Port Vila and (right) Luganville locations.

3.1.2 Van-KIRAP Ocean Buoys

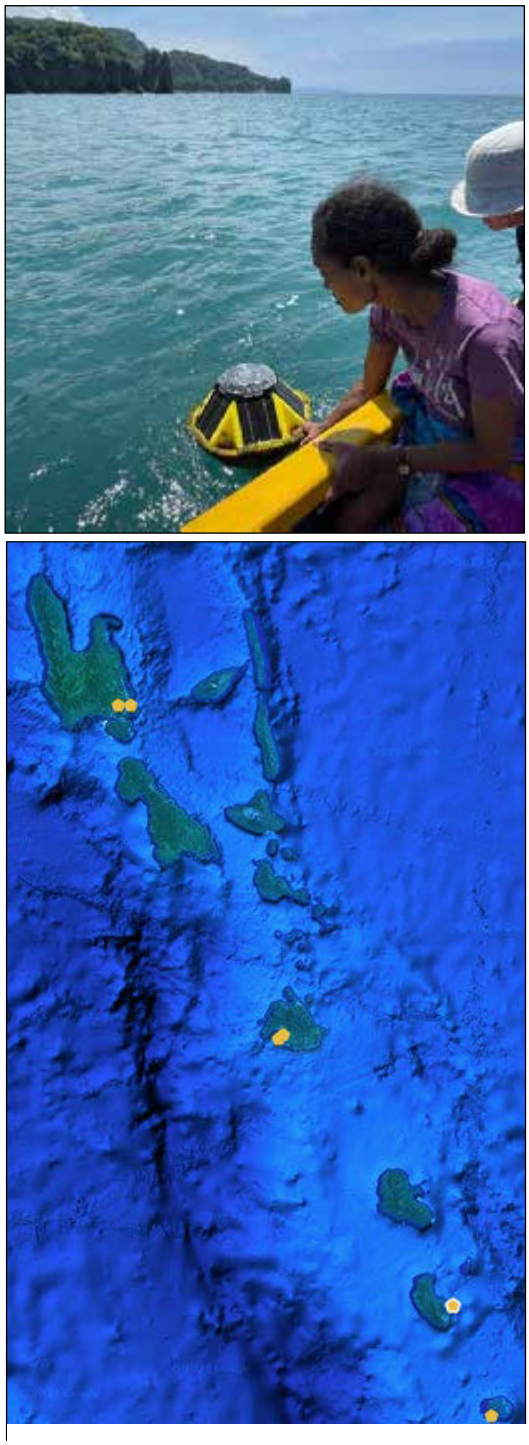

Figure 12: A Sofar Spotter being deployed off Port Resolution, Tanna on 11 October 2022 (top). Ocean Observing (Spotter) buoy network locations as of April 2023

A World Meteorological Organisation (WMO) and the Intergovernmental Oceanographic Commission (IOC) of UNESCO workshop in 2021 (https://www.spc.int/updates/blog/2021/06/pacific-islands-call-for-coordinated-regional-approach-to-ocean-observing) stated that "In the Pacific, ocean observations provide critical information to a wide range of key economic sectors such as fisheries, pearl farming and aquaculture, maritime transport and tourism, as well as coastal early warning systems … existing national ocean monitoring programmes were not sufficient to match their needs." It also noted that "Weather and climate models are run at a global level and our models are only as good as the data we feed them with." This confirms conclusions in multiple other reports and publications that existing *in situ* ocean monitoring, particularly of ocean waves and water levels, is insufficient for many applications, especially as related to ocean and coastal hazards (e.g. Hoeke et al., 2013; Iwamoto et al., 2016; Wandres et al., 2020).

This is true of Vanuatu, where no long-term monitoring of ocean wave, temperature or acidification (OA) has historically occurred or was planned for at the inception of the Van-KIRAP project. Following capacity building and consultation supported by this activity, Van-KIRAP project management approved procurement of six Sofar Spotters (https://www.sofarocean.com/products/spotter), a new-technology, small, lightweight type of buoy which measures ocean waves and temperature and transmits its data as well as other water level and OA monitoring equipment. Through coordination between VMGD and the Fisheries Department, the Spotters were subsequently deployed September – December 2022, establishing Vanuatu's first ocean monitoring network (Figure 12). Subsequently another three buoys have been requisitioned; buoy mooring guidelines (Martini, et al. 2021, https://doi.org/10.25919/vy0b-zh52). Furthermore, a customised software dashboard to support better use of Spotter buoy and other coastal instrumentation data (both developed by the CSIRO team), together with a capacity building and training programme, has been established to develop a proper data management plan and to ensure longevity of the deployed system.

Unfortunately, since the Spotters were not deployed until 2022, they were not available for the initial tuning periods and sensitivity tests. However, additional simulations of the ocean-hazard modelling system were performed covering several of the Spotter deployment periods.

Comparison statistics for two of the buoys are shown in Table 4; Figure 13 shows a detailed comparison of ocean wave variables simulated by the modelling system and the Spotter Buoy deployed near Million Dollar Point, Luganville, showing excellent overall agreement between the model's simulated output and observations.

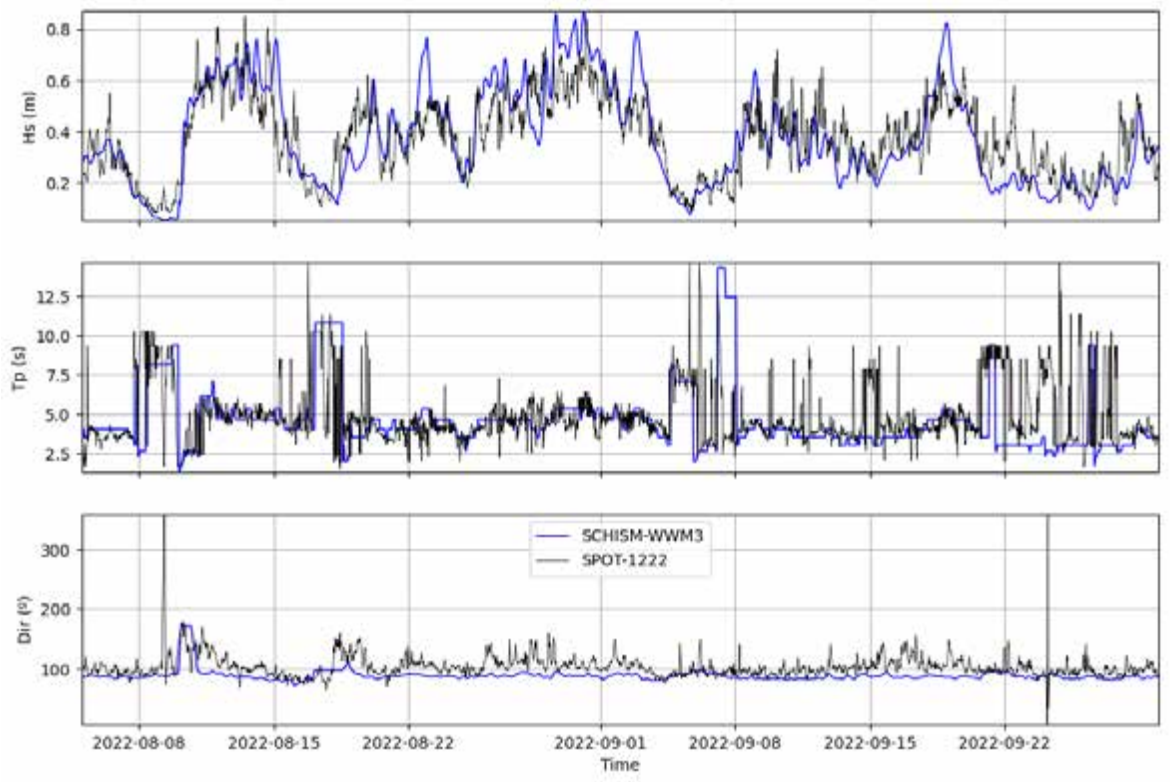

Figure 13: Comparison of key ocean wave variables simulated by the modelling system and the Spotter Buoy deployed near Million Dollar Point, Luganville (SPOT-1222).

3.1.3 Hindcast vs Satellite data

Satellite wave data has been extracted from the Australian Integrated Marine Observing System (IMOS) AODN database (https://portal.aodn.org.au/), which consists of significant wave height (Hs) and wind speed from 13 altimeters starting in 1985. It provides the information for all the different altimeter missions under the same format, on a regular grid of 1° worldwide. The IMOS database has been selected as it has been calibrated against multiple world-wide buoy observations as well as cross-validated with altimeters to test for consistency (Ribal & Young, 2019).

The altimeter data provided by IMOS covers the period from 1985 to 2020, except for the lapse between 1990 and 1991 when no satellite missions were deployed. For the analysis provided in this work, the whole database has been used. Figure 14 shows the durations of altimeter data in the database from all satellite missions.

Since the spatial resolution of the satellite wave heights are far coarser than those of the Van-KIRAP national ocean-hazard modelling system, outliers may occur in the comparison with the hindcast where wave dynamics within the model are of much finer-scale than those resolved by the satellite altimeters. To ameliorate this, a range of different filters to differentiate outliers from

the altimetry database have been used and single value statistics comparing the hindcast with altimetry have been omitted from Table 4. Instead, in this section, we focus on large-scale spatial comparisons.

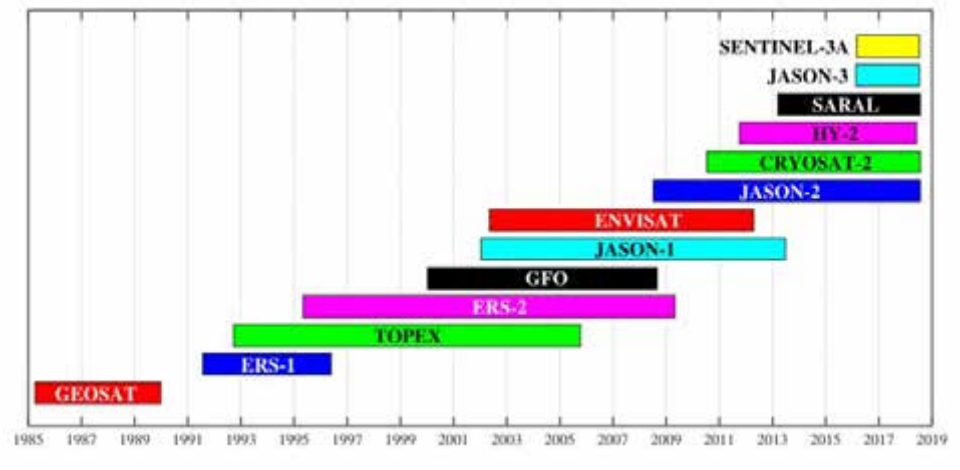

Figure 14: Durations of altimeter data in the database from all satellite missions (from Ribal & Young, 2019).

Figure 15 shows the excellent agreement between the Hs from the hindcast and from the satellite database for given times along the corresponding satellite tracks. This figure shows the data in a scatter plot along longitude-significant wave height axes (left panel) and on a map (right panel) that displays the hindcast wave height field and the values of the satellite database (track). Figures 16-19 show the equivalent graphs to the previous figure for the available times that coincide with the occurrence of TC Harold in April 2020 (Figure 16 and 17) and TC Pam in March 2015 (Figures 18 and 19). Figure 20 shows the overall Root Mean Square Error (RMSE) between the satellite and hindcast Hs for a 4.5-year period showing that with the exception of a few isolated satellite tracks, RMSE differences in wave heights are generally between 0.2 m and 0.4 m, including during TC events.

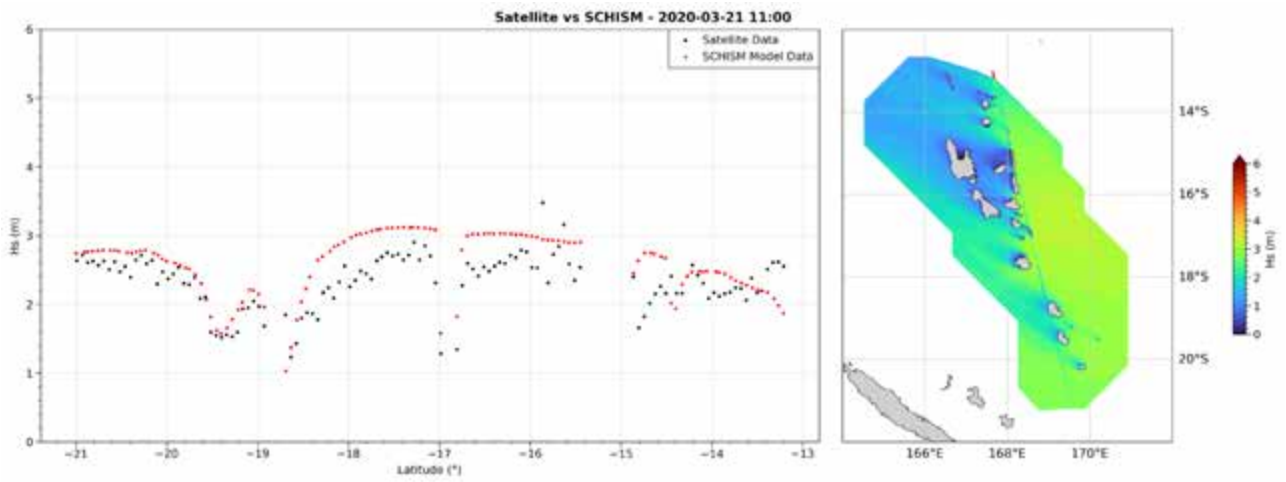

Figure 15: a) Verification of significant wave height values for 2020-03-21 11:00 UTC with satellite values; b) the satellite track (coloured circles within the domain; red circles outside) shown over the SCHISM-WWM3 significant wave height data.

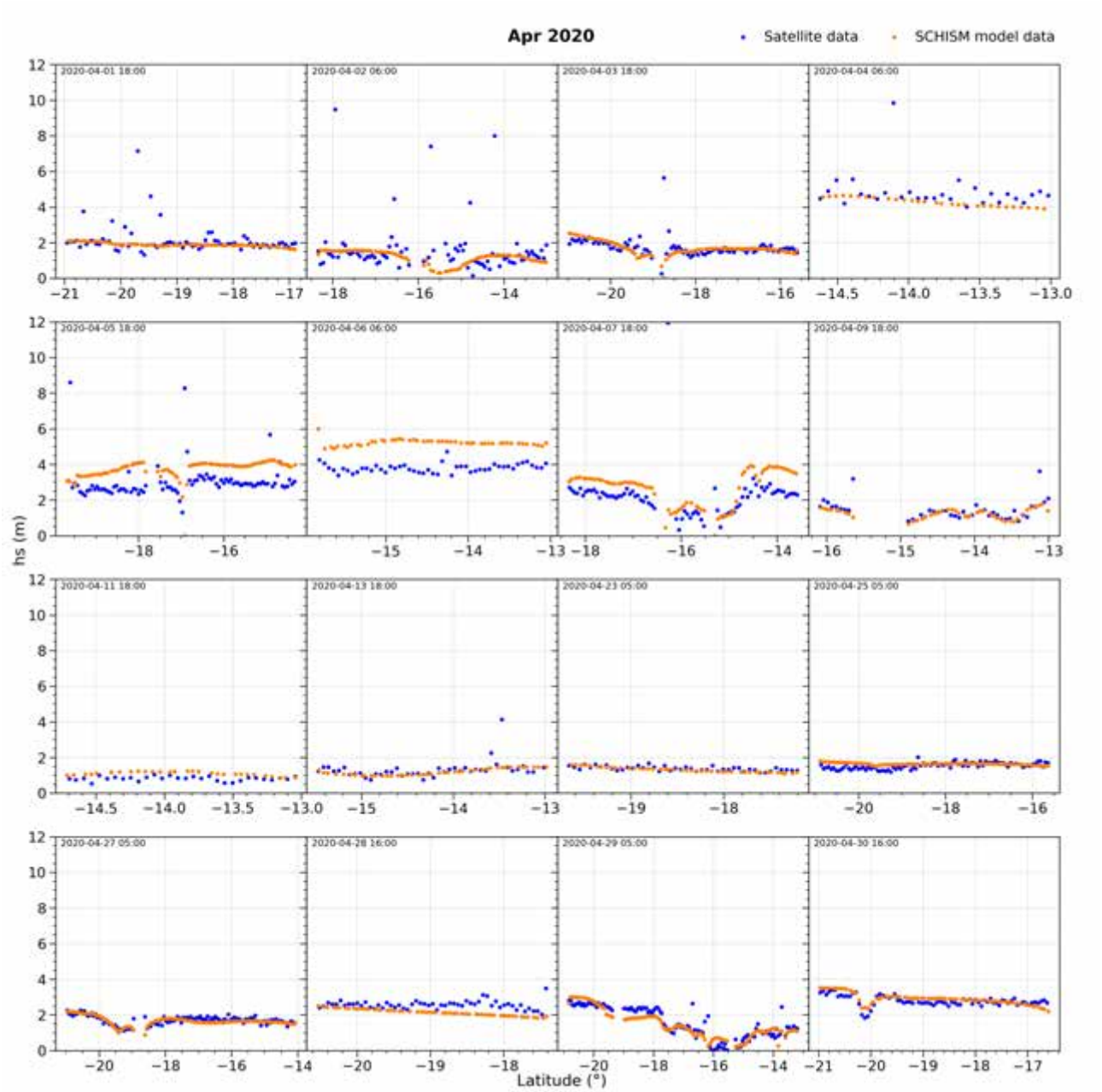

Figure 16: Verification of modelled significant wave height values (red circles) with satellite data (blue circles) for TC Harold.

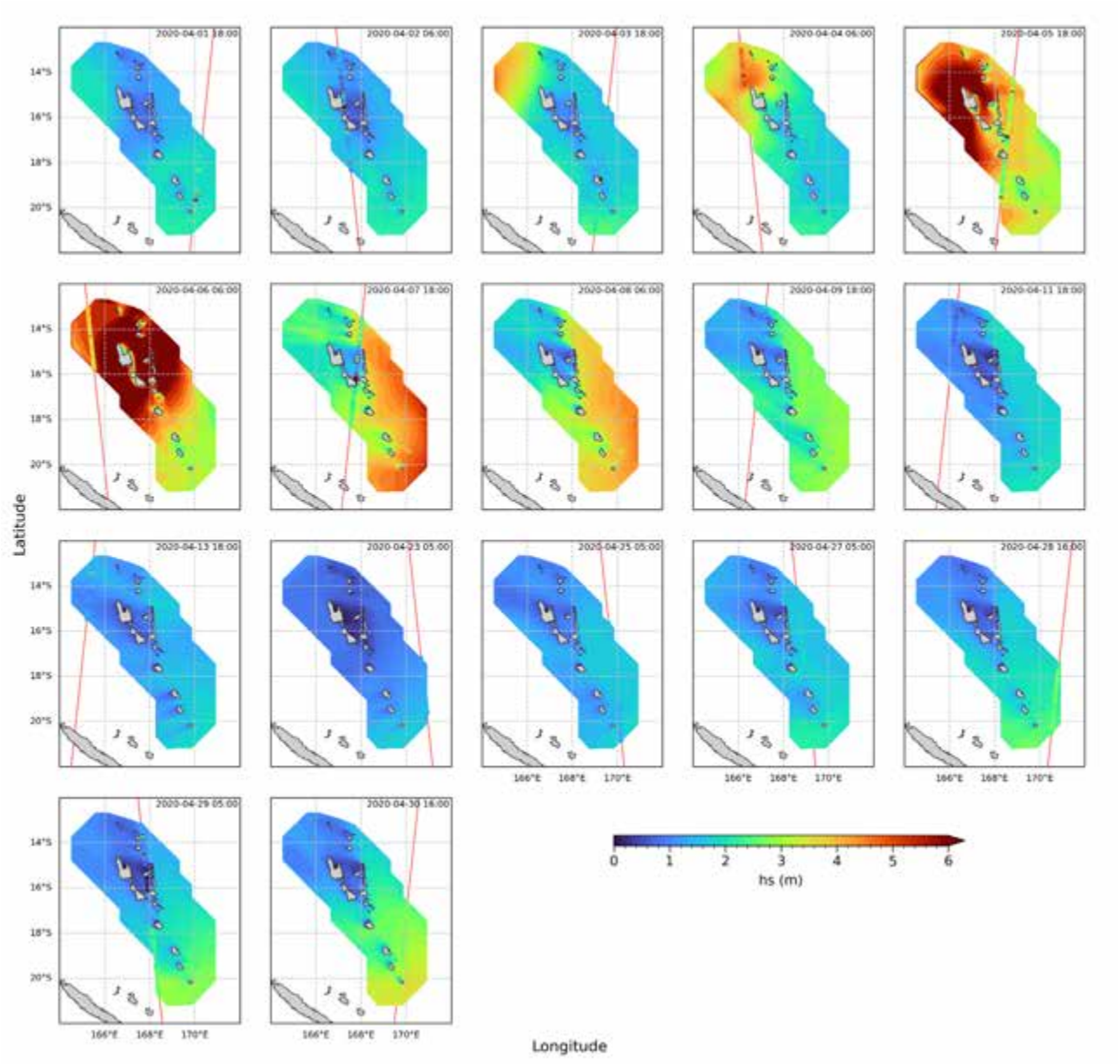

Figure 17: Verification of modelled significant wave height values (background field) with satellite data (coloured circles along the satellite track) for TC Harold

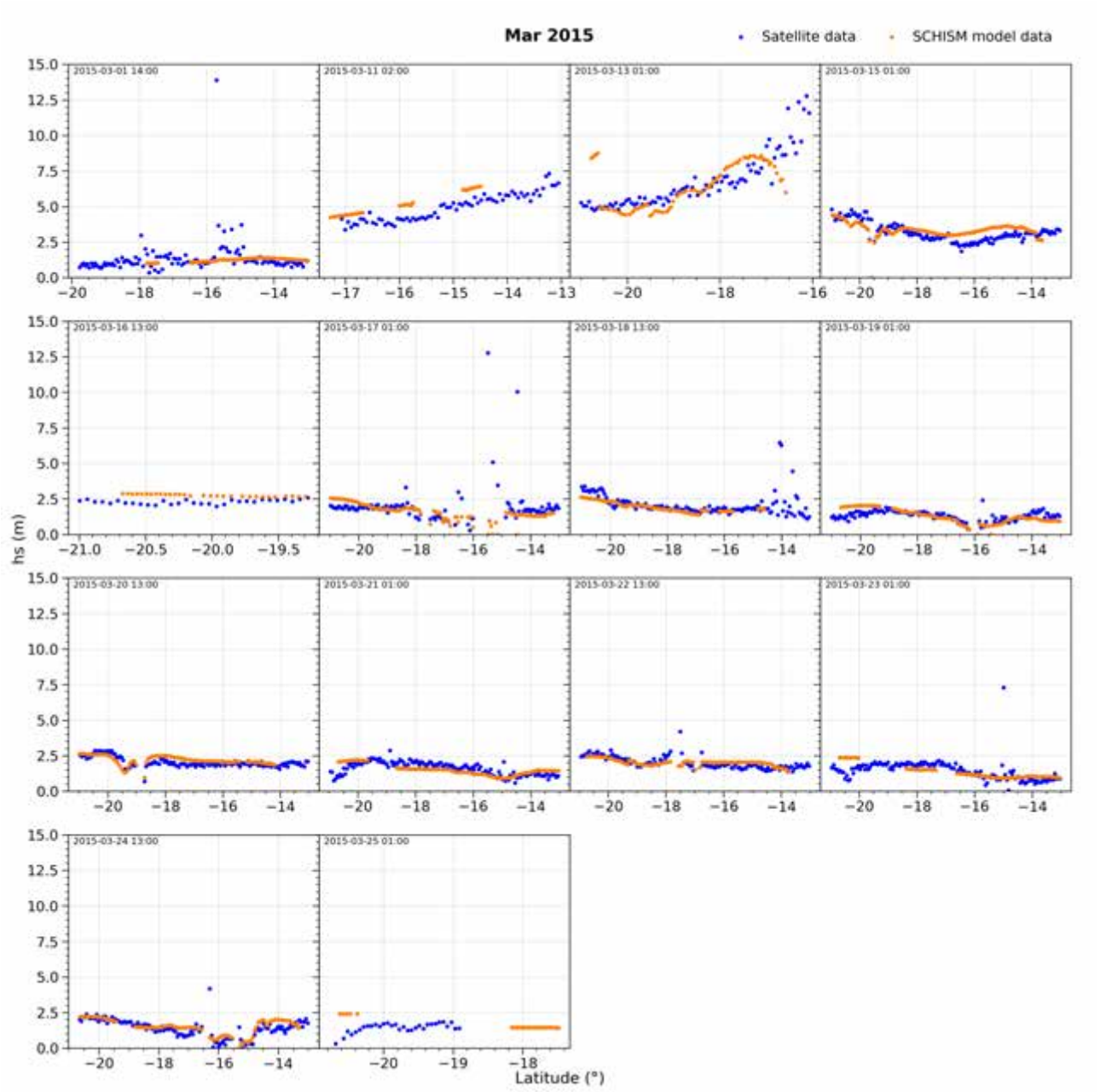

Figure 18: Verification of modelled significant wave height values (red circles) with satellite data (blue circles) for TC Pam

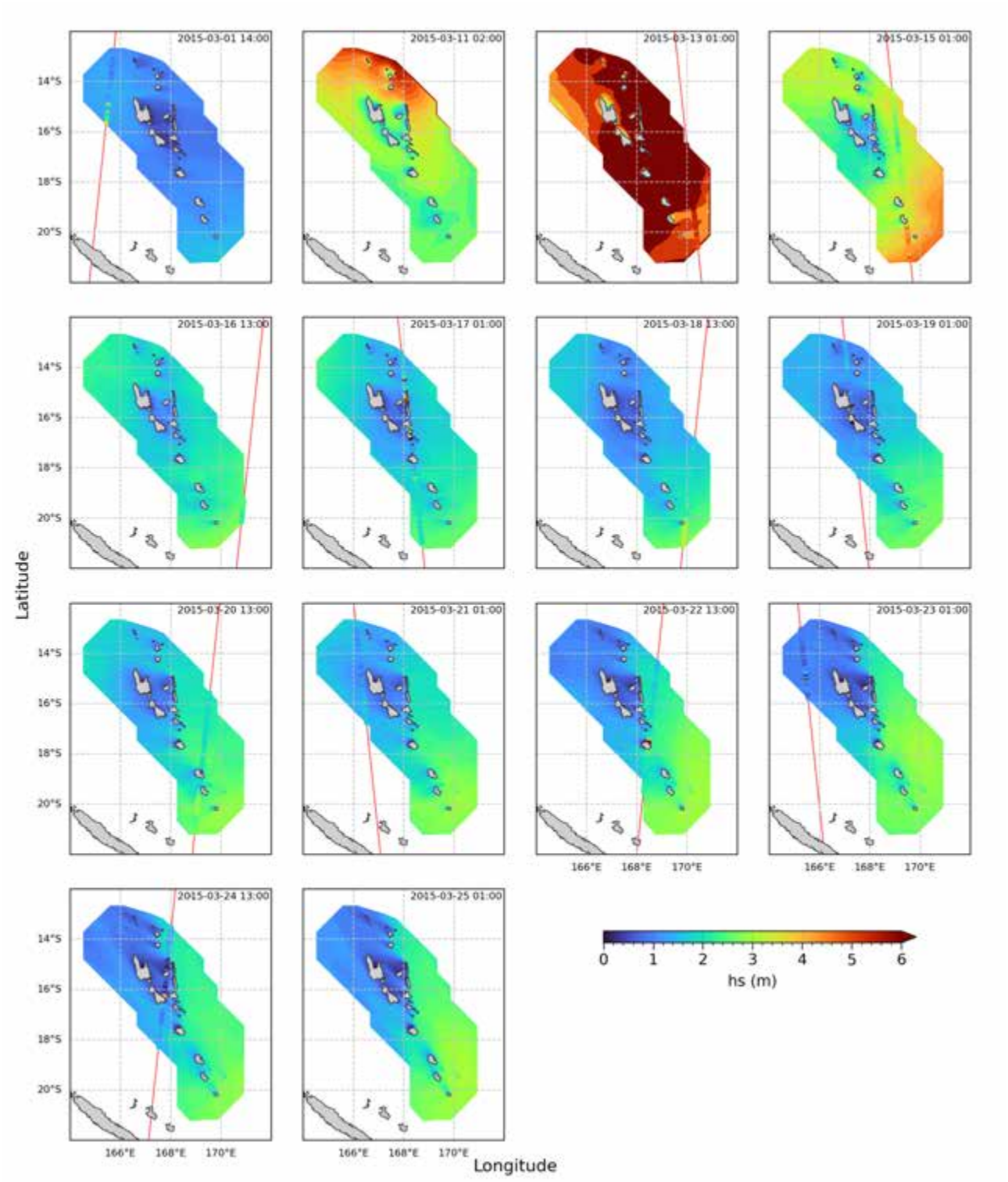

Figure 19: Verification of significant wave height values with satellite data (coloured circles along the satellite track) for TC Pam.

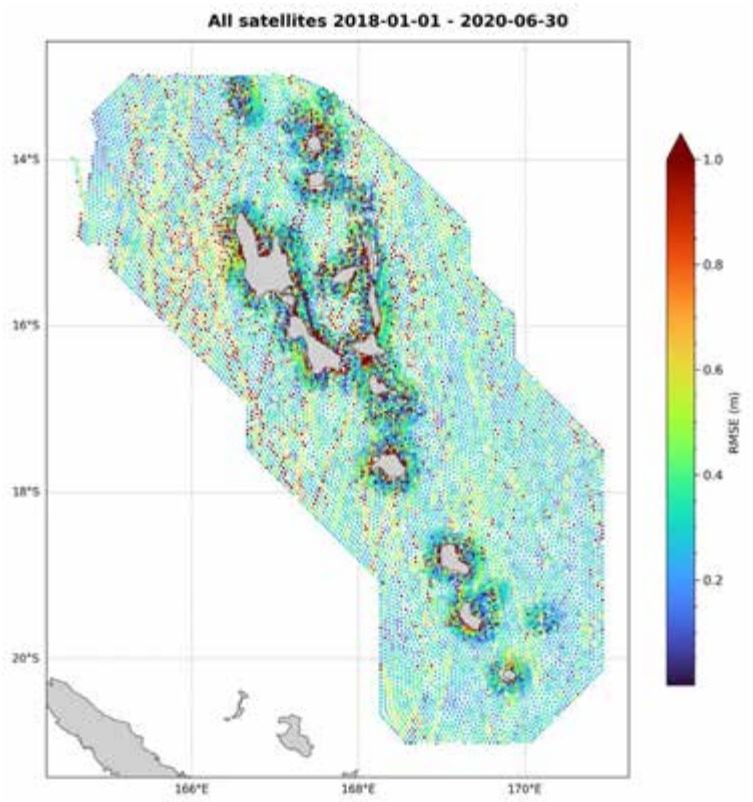

Figure 20: RMSE results from the comparison between satellite data and hindcast data.

4 Ocean-hazard modelling system: Probabilistic Tropical Cyclone assessment

In regions such as Vanuatu, statistically rare, but high-impact TCs tend to dominate extreme sea level events and related coastal flooding. As described in Section 1.3.2, any particular location has likely been significantly impacted by a TC only a handful of times in the last 20-40 years, which is the time span covered by tide gauges and the historical hindcast described in the last section. This translates to very high statistical uncertainties for extreme value analysis, which makes it difficult or impossible (for instance) to predict a meaningful 50-year storm tide or storm wave height (see Figures 5 and 6). Probability-based estimates of extremes such as these are required for successful coastal planning and adaptation and excessive statistical uncertainty can led to poor decisions and maladaptation. To overcome these high statistical uncertainties, previous assessments have often used stochastically generated synthetic populations of thousands of TCs, to reduce statistical uncertainty in TC impacts (for examples, see Lin et al., 2010; McInnes et al., 2011). This section describes our use of synthetic TCs in conjunction with the national ocean-hazard modelling system.

We take advantage of synthetic TC populations developed for Vanuatu within the Van-KIRAP Climate Projections (1.2.3) activity. These are based on the MIT synthetic track model (Emanuel et al., 2006, 2008), see “Box 5” in the Van-KIRAP “National and sub-national climate projections for Vanuatu“ final report (Kirono et al., 2023). We use the historically based NCEP/NCAR (https://rda.ucar.edu/datasets/ds090.0/) based synthetic TC population and define TCs with potential to affect Vanuatu as those with tracks that pass within a circle with a radius of 8° of Latitude centred on Vanuatu. Figure 21 shows the number of historical and synthetic TC tracks which intersect this 8° circle; the historical tracks are sourced from International Best Track Archive for Climate Stewardship (IBTrACS Version 4, https://doi.org/10.25921/82ty-9e16, Knapp et al., 2010). There are 108 historical TCs meeting this definition, compared to 3,852 synthetic TCs.

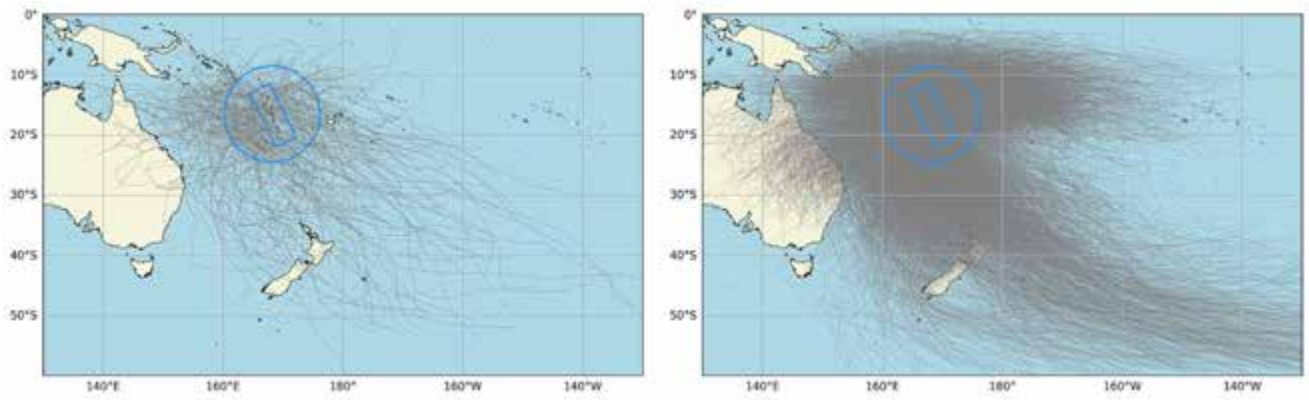

Figure 21: (left) the 108 historical (IBTracs) TC tracks and (right) the 3,852 synthetic TC tracks crossing the 8º circle centred in Vanuatu.

Simulating storm surge, storm waves, tides and background sea level for all 3,852 synthetic TCs using common downscaling dynamic approaches would come at an unrealistically high

computational cost. Furthermore, it would be unable to randomly sample the different TCs occurring at different stages of tide or sea level. Therefore, a hybrid model framework TC emulator, which combines the numerical (dynamic) downscaling with statistical techniques together with numerical modelling and Monte Carlo (probability) simulation, was developed. The details of this framework are presented in the following sections.

4.1 TC parameterization and ShyTCwaves

Since the study site of Vanuatu encompasses a large domain of many islands a parameterization has been implemented to take into account all plausible TCs incoming directions while applying the hybrid model predictive tool. For this purpose, two areas of influence were defined around Vanuatu: (a) the 8° radius circle (ellipsoid) centred over Vanuatu and (b) a rectangle containing all the land territory of Vanuatu, which also corresponds to the national ocean-hazard modelling system extent (Figure 22). TC information was then parameterised, in order to preserve the key TC track characteristics when approaching, passing over and exiting of the Vanuatu area. Both samples of historical (IBTracs) and synthetic TCs were parameterized in terms of:

(1) *Pmin*, the minimum central pressure along line P1-P2;

(2) *Vmean*, the mean translation velocity along line P1-P2;

(3) *Gamma*, the angle track of direction along P2-P3;

(4) *Delta*, the azimuth of the entrance point in the rectangle;

(5) *dP_0* the absolute changes of *Pmin* of the lines P1-P2 compared to P2-P3

(6) *dV_0* the absolute changes of *Vmean* of the lines P1-P2 compared to P2-P3

(7) *dG_0* the absolute changes of *Gamma* of the lines P1-P2 compared to P2-P3

(8) *dP_2* the absolute changes of *Pmin* of the lines P3-P4 compared to P2-P3

(9) *dV_2* the absolute changes of *Vmean* of the lines P3-P4 compared to P2-P3

(10) *dG_2* the absolute changes of *Gamma* of the lines P3-P4 compared to P2-P3

This more complex parameterization (compared to e.g. van Vloten et al., 2022) allows for greatly improved characterization of complex and/or regionally tangential TC tracks, such as those that double back through the region like TC Oma in 2019. Once all TCs were parameterized, a representative selection of 1,000 TCs from the 10-dimension parametric space were identified using the Maximum Dissimilarity Algorithm (MDA) which includes extreme values of the parametric data (Figure 23). Due the nature of MDA, the 1,000 cases are the best optimized representation of the parameter space (Camus et al., 2011), therefore providing an ideal “design storm” database of TC members for simulation with the national ocean-hazard modelling system.

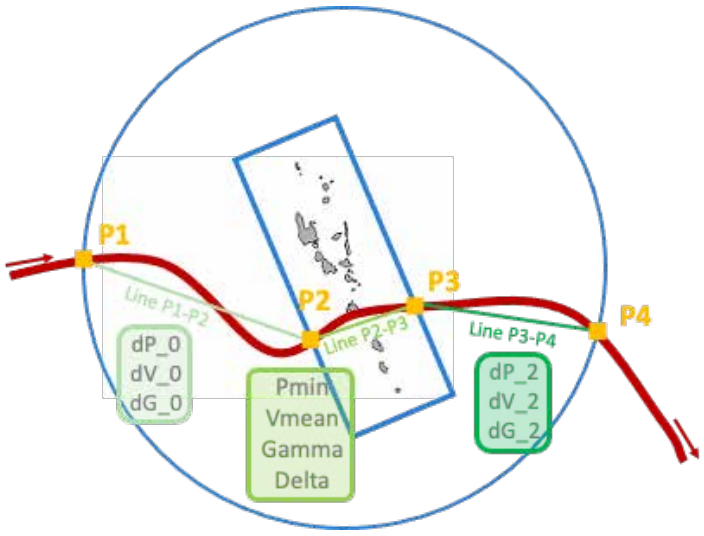

Figure 22: Parameterization of a TC track over Vanuatu into three lines within the circle and rectangle influence areas.

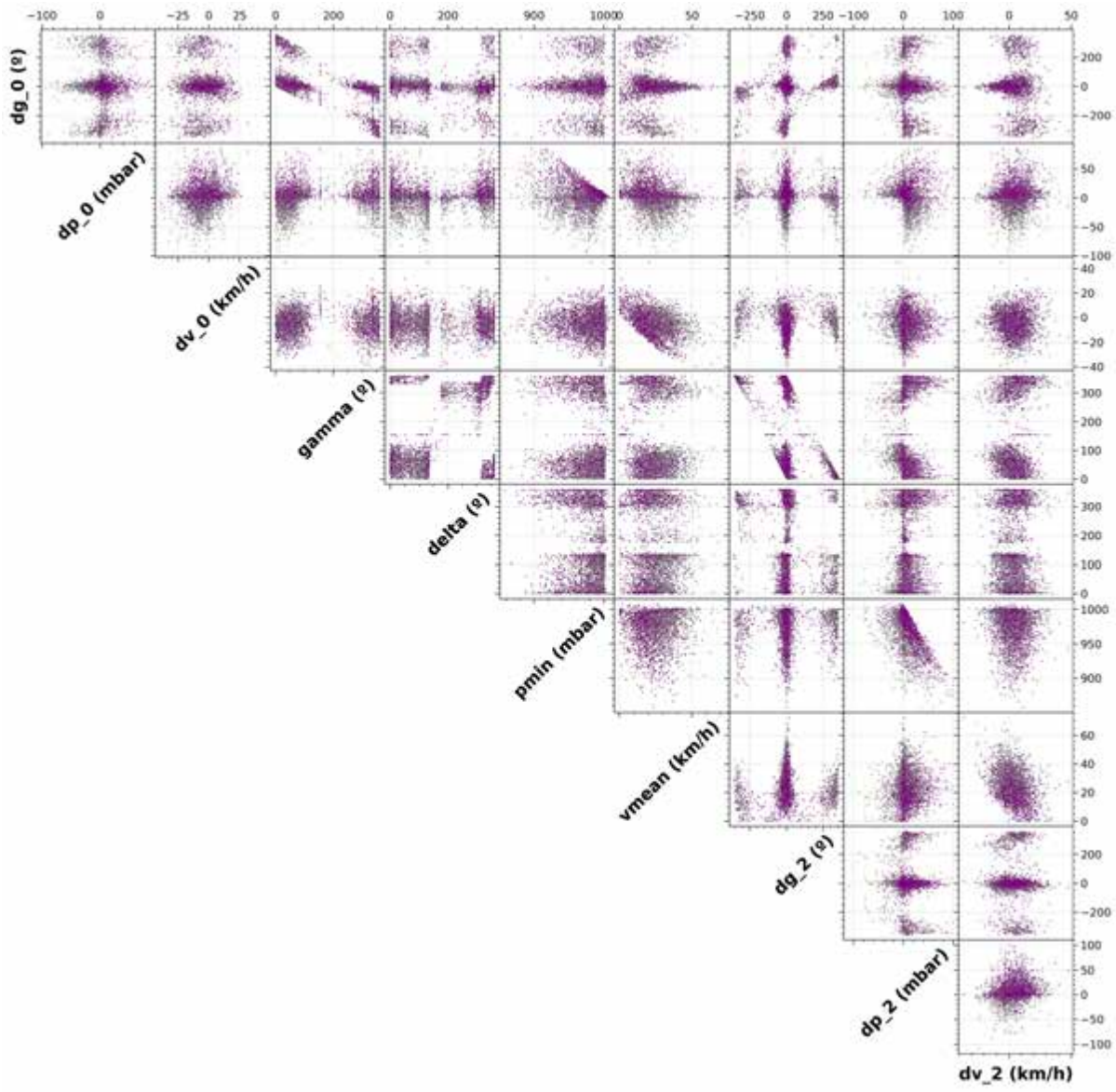

Figure 23: Multidimensional depiction of TC parameter distribution of all members of the TC data set (grey points) and the MDA-selected case (purple points).

A key challenge in simulating the 1,000 MDA selected TCs is wave boundary conditions. Unlike the historical hindcasts, the synthetic database TCs are not associated with a larger global or regional simulation of waves, which can propagate long distances, well outside of and into the ocean hazard model domain (e.g. Hoeke et al., 2021). To overcome this, the metamodel SHyTCWaves (van Vloten et al., 2024) has been used to obtain wave boundary conditions to force the ocean hazard model for each of the 1000 representative TCs. This metamodel provides time-varying directional wave spectra along the domain of Vanuatu (Figure 24). SHyTCWaves consists of splitting a TC track into segments of 6 hours, with reconstruction of the spectra at each boundary point using analogue segments from a precomputed library of 5,000 segments.

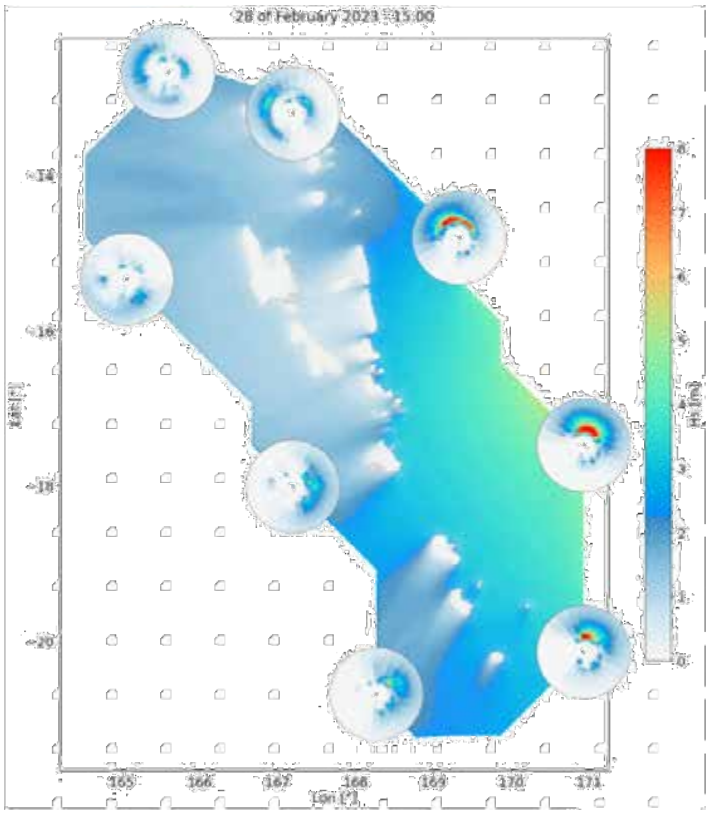

Figure 24: Example of the hydraulic boundary conditions in deep waters (directional wave spectra) along the domain of Vanuatu at a given time obtained through SHyTCWaves metamodel.

The atmospheric (wind and pressure field) forcing was generated using an asymmetric, modified Holland vortex (Fleming et al., 2008; Holland et al., 2010), based on the time-varying track, central pressure, translation speed and radius of maximum winds available for all TCs within the 1,000-TC MDA database. Water level boundary conditions (tides and background sea level) were held at zero (current mean sea level); they are re-sampled separately later, as discussed in the following sections.

4.2 Emulator of TCs

The national ocean hazard model simulations described above resulted in a precomputed library of high-resolution, time varying storm surges (SS) and storm waves, each associated with the

passage of the 1,000 synthetic TCs. This library has been used to generate Monte Carlo time series of total water levels (TWLs), which include tides and background sea level variability. The following analyses and pre-processing were performed to develop the requisite Monte Carlo emulator:

- The historical TCs (IBTrACS) that cross the 8º ellipsoidal influence area during the period 1980-2020 (see Figure 21) is used to calculate the mean number of TCs (3.5) per year.
- The joint probability density function (PDF) of these TCs by category (Pmin inside the 8º ellipsoid using the Saffir-Simpson scale) and by month is calculated (Figure 25).
- The parameterized TCs database is sorted in terms of the TC category (Pmin inside the ellipsoid), generating indices for TCs of each category.
- Each 3,852 TCs from the synthetic TC population is assigned with the corresponding MDA analogue index (defined by those TCs closest in the 10-dim parametric space Euclidian distance to the MDA sub-set) which will be used instead.

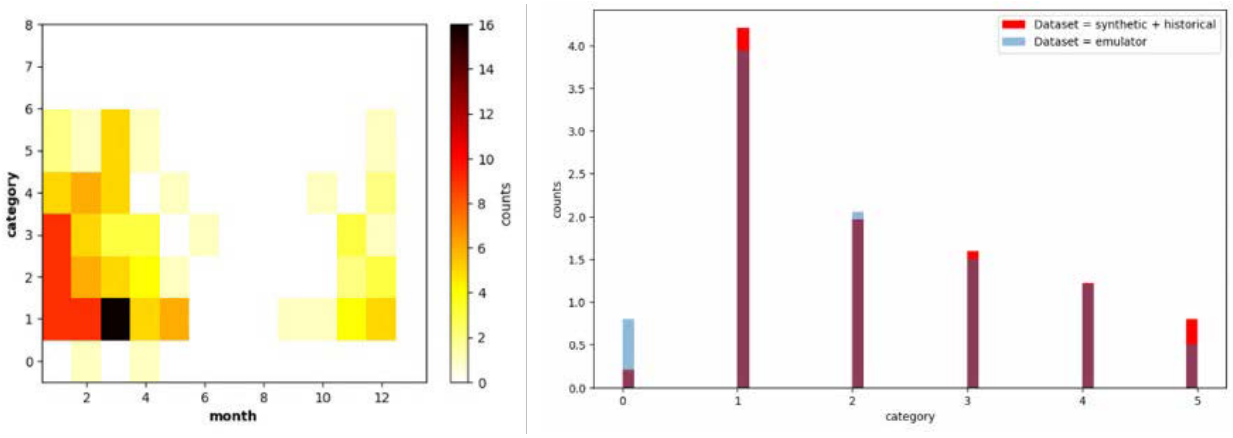

Figure 25: (left) joint PDF of historical TCs crossing 8º circle, by month and Saffir-Simpson scale category; and (right) comparison of annual mean distribution of TC categories within the synthetic+historical database and that produced by the emulator.

The generation of synthetic series of TWL is then computed as a Poisson-process controlled summation of the contributions of:

- Monthly mean sea level (MMSL) variability, from ORAS5 with geodetic correction (the same as used to force the historical hindcast, stored in coastal points
- Astronomic tide (AT), from one year (2020) simulation by the national ocean hazard model
- Waves+SS, from 1,000 parameterized TCs by the national ocean hazard model

The Monte Carlo simulation (i.e. 10,000 years) is generated with the following steps:

- Poisson distribution with mean parameter (3.5 TCs per year) generates the number of TC events that occur in each i^{th} year.

Figure 25 (right) shows the comparison of the distribution of counts of TC categories between the original dataset (historical and synthetic TCs crossing the 8º radii circle and parameterized) and the Monte Carlo emulator.

The following steps apply for each event:

- A random number selects the TC category$_i$ and the month$_i$ (using the PDF) --> a TC with category$_i$ from the MDA is selected. For each relevant computational node in the national ocean hazard model, the date-time with maximum waves+SS is selected
- A random number selects the year$_i$ between 1980-2020 (MMSL, ORAS5) --> the MMSL is extracted for year$_i$ and month$_i$ (constant for all computational nodes)
- A random number selects the day$_i$
- A random number selects the hour$_i$ --> the AT at day$_i$ and hour$_i$ is centred to coincide with the datetime with maximum waves+SS for each computational node
- The TWL is computed as MMSL + AT + (waves+SS)

Figure 26 shows an example of the results obtained for the synthetic series of TWLs.

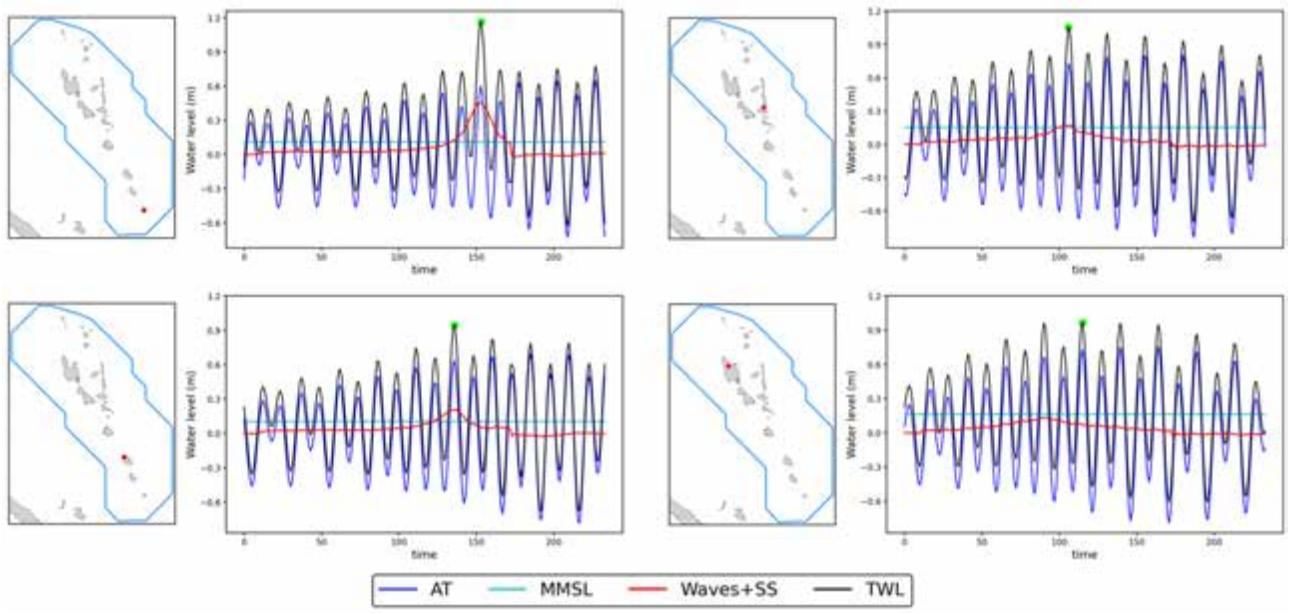

Figure 26: Example of synthetic series for one random TC event at several computational nodes near the coast.

The generation of synthetic series of TWLs assumes that the linear addition of its components does not introduce significant error, i.e. that tides and sea level can be linearly added to separately simulated waves and SS (TWL = [wave processes + SS] + tides + MMSL). This linear assumption was tested by comparing several TC simulations within the 41-year hindcast (all of which consists of dynamically coupled wave processes + SS + tides + MMSL) to simulations of [wave processes + SS] with linearly added to pre-computed tides and MMSL. Figure 27 shows the results of one of these comparisons at the Port Vila location. Figures 28 and 29 show maps of TWL fields for two given times from the hindcast and from the linear summation of components simulated separately.

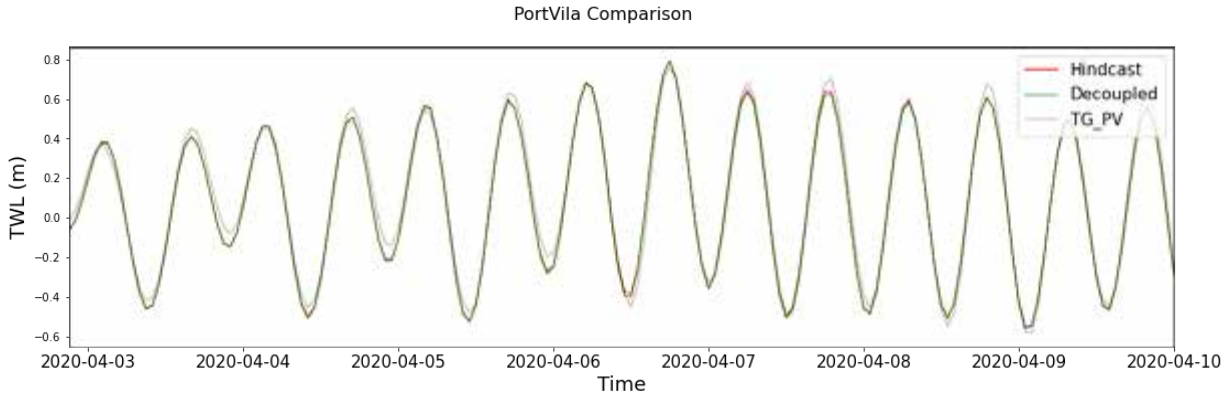

Figure 27: Comparison between the TWL result of the hindcast (coupled) and linear summation of the components (astronomical tide, storm surge and waves) simulated separately (decoupled) at Port Vila location.

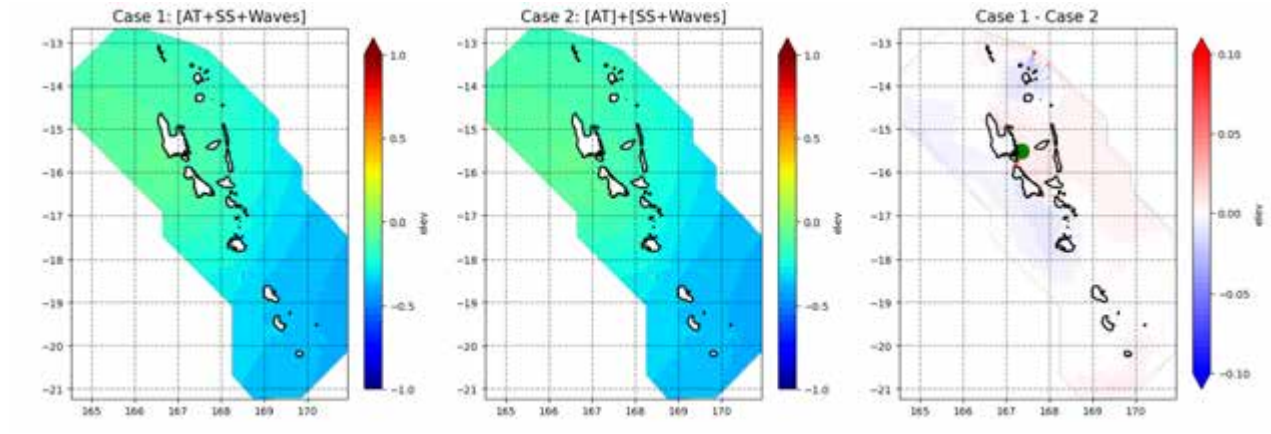

Figure 28: Maps of TWL for a given time from the hindcast (where wave processes + SS + tides + MMSL are dynamically simulated together, case 1 at left); from a dynamical simulation [wave processes + SS] with tides and MMSL linearly added (case 2, centre); and the difference between case 1 and case 2.

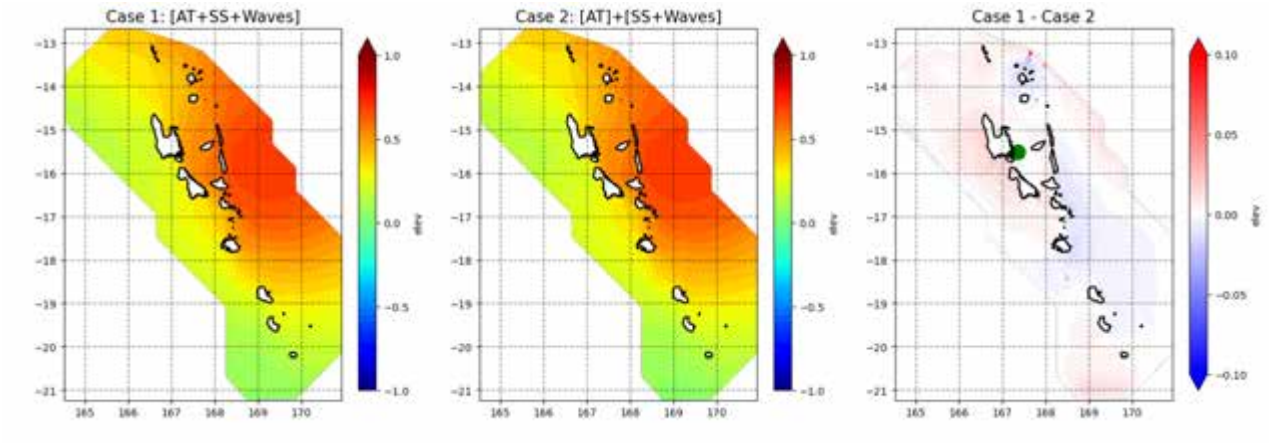

Figure 29: Similar to Figure 28, maps of TWL fields for a different time from the hindcast (case 1 at left); from a dynamical simulation [wave processes + SS] with tides and MMSL linearly added (case 2, centre); and the difference between case 1 and case 2.

5 Risk-based mapping using the national extreme sea-level assessments

In this section, we describe the extreme value analyses (EVA) applied to output from the National Ocean Hazard Model historic (41-year Hindcast) “mode” and probabilistic (Monte Carlo TWL) “mode” outputs; how these EVA results are combined with SLR to produce projected extreme sea level return period probabilities; the data formats and how they are utilised to produce inundation layers within the Van-KIRAP Climate Information Services (CIS).

5.1 EVA of the historic mode

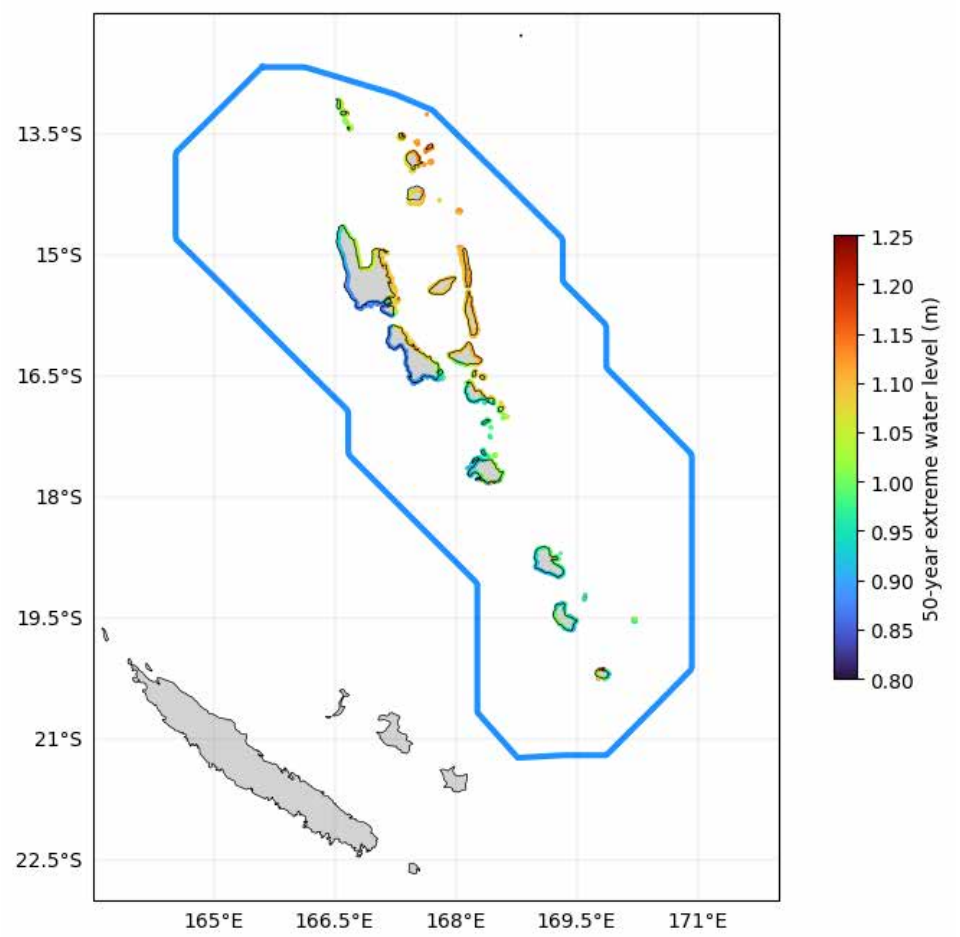

Figure 30: Coastal points at regular 2km spacing throughout Vanuatu used for near-shore extreme sea level analysis within the National Ocean Hazard Model domain (indicated with a blue outline). Colours of coastal points indicate the 50-year extreme water level derived from EVA of the 41-year hindcast.

To support meaningful extreme value analysis (EVA) of extreme total water levels (TWLs) near the shoreline, a series of 2331 coastal points at 2 km spacing around all islands in Vanuatu was created (Figure 30). 41-year hindcast hourly water levels from the Ocean Hazard Model’s nearest “wet” computational nodes were nearest-neighbour interpolated to these points. A generalised Pareto distribution (GPD) fit to peaks-over-threshold extremes approach (Coles, 2001) was applied, using a local (coastal-point specific) threshold value of the 99.5 TWL percentile. Additionally, a 60-hour

window was used to de-cluster the event data, to prevent two successive semi-diurnal tidal peaks (daily higher-high tide events) to be counted as two separate events. This overall EVA approach allowed local (empirical and GPD fitted) return periods to be calculated, including extrapolating beyond 41 years for GPD fitted return periods. This is shown for an example coastal point in Figure 31.

While consideration of extreme sea level return periods generally only make sense along the shoreline, extreme wave heights can be considered across the entire model domain, where they may (for example) impact offshore reefs and fishing or other operations. The same EVA analysis described for the historic coastal TWLs was applied to wave heights for all the "wet" computational output points. This is shown in Figure 32.

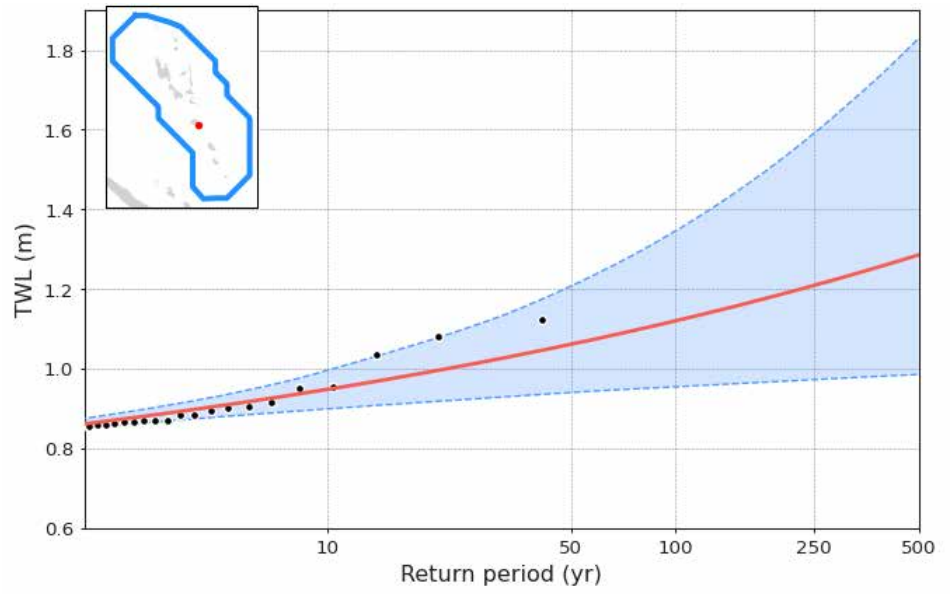

Figure 31: Total water level (TWL) return periods derived from the Ocean Hazard Model historic mode for a coastal point on south-east Efate Island. The black dots represent the empirical return periods of actual events in the hindcast; the red line and blue bands are the statistical (GPD) fit and associated uncertainty (95% confidence limits). The location of the coastal point is indicated with a red dot in the inset map at the upper left (the perimeter of the model domain is indicated in blue).

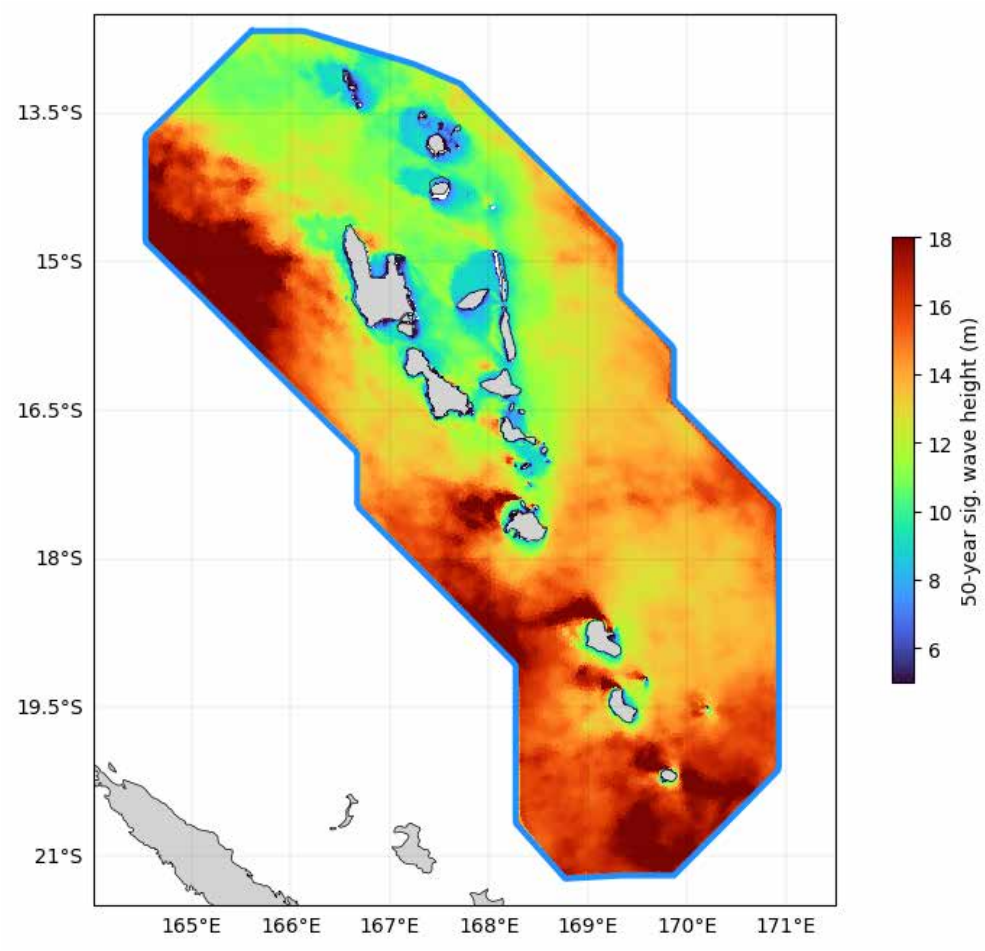

Figure 32: 50-year return period of significant wave height derived from the Ocean Hazard Model historic mode.

5.2 EVA of the probabilistic mode

Due to the Monte Carlo approach described in Section 4.2, the probabilistic mode produces hundreds of thousands of potential combinations of storm surge, storm waves, tides and sea level, ("synthetic series", see Figure 26 for an example) which equates to approximately 10,000 years of TCs at the current/historical average rate of TC occurrence in Vanuatu (3.5 TCs per year occurring within the 8º radius circle). Therefore there is no need to fit the extreme TWLs and waves simulated by the probabilistic mode to one of the generalized extreme value (GEV) family of distribution functions (such as the GPD fitting used in the last section), since such EVA extrapolation techniques are only necessary when the time range of the available data is shorter than the required return period value estimates (which is the case, for example, when estimating 50 and 100-year return periods from the 41-year historic mode hindcast). Instead, we apply an EVA methodology conceptually similar to Van Vloten et al. (2022). For the TWLs, the same coastal points described in Section 5.1 and shown in Figure 30 are used. The TWL synthetic series at each coastal point are then arranged into 10 portions (of "ensemble members") representing 1000 years each and the annual maxima of each member computed, allowing estimation of uncertainty in the results. The empirical return periods are then calculated for each ensemble member; see Figure 33 for an example coastal point's return periods.

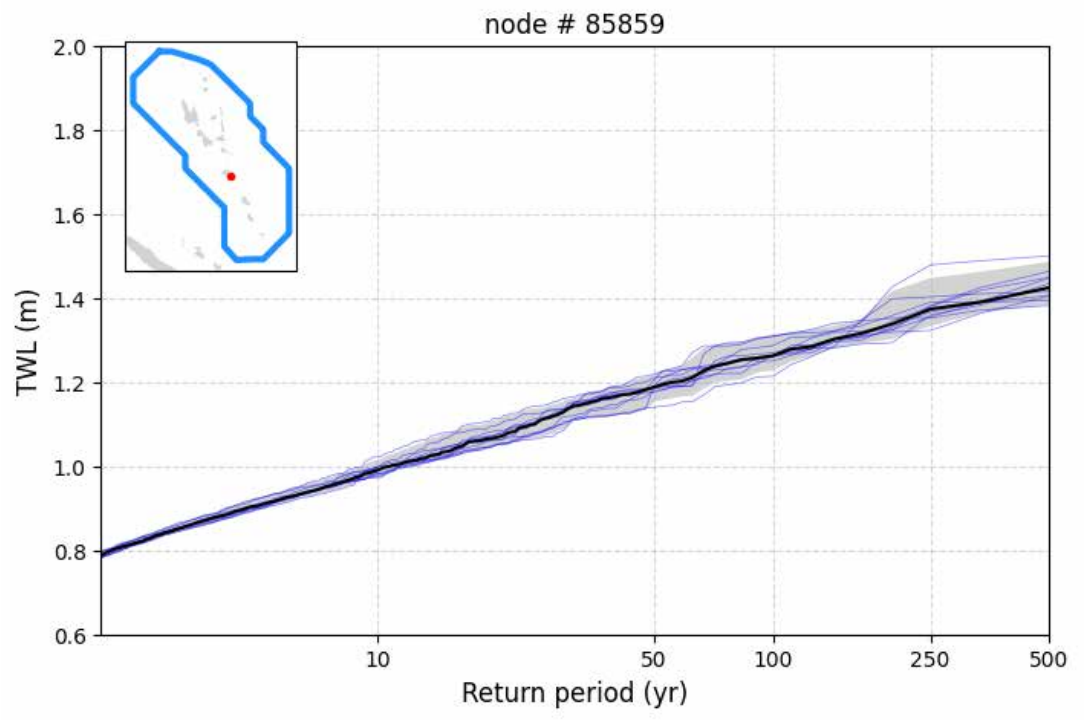

Figure 33: Total water level (TWL) return periods derived from the Ocean Hazard Model probabilistic TC mode for a coastal point on south-east Efate Island. The heavy black line is the median ensemble value of the empirical return periods (based on the synthetic series described in section 4.2); the grey area around the black line and fine blue lines are the 90% ensemble confidence limits and individual ensemble empirical return periods, respectively. The location of the coastal point is indicated with a red dot in the inset map at the upper left (this is the same location as represented in Figure 30).

For evaluation of TC-related probabilistic extreme wave heights across the entire modelling domain, we neglect the coincident emulation of tides, sea level and storm surge that was performed at the coastal points for TWL. While this may lead to relatively slightly higher uncertainty in wave height return periods in very shallow water parts of the model domain (as tide and sea level will modify wave heights in shallow areas), this is dynamically captured to some degree in the coastal point TWLs (which includes wave processes) and will make no difference in the deeper water parts of the model. We consider this an effective trade-off which reduces complexity and computational effort for probabilistic extreme wave height return periods. To create them, a similar series of 10 ensemble members of TCs, representing 1000 years (also based on the Poisson distributions in Figure 26) was drawn from the synthetic (probabilistic) TC Ocean Hazard Model database simulations (but further emulation of coincidence with tides and sea level is neglected). The maximum (significant) wave height for each year at each model computational node can then be calculated and empirical return periods are then calculated for each ensemble member. This is conceptually similar to the maximum wave "swath" approach taken by van Vloten et al., (2022). The median value and the 90% confidence limits of the return periods of the wave height ensemble are treated the same way as for the TWL ensembles. Figure 34 shows the 50-year return period wave height as an example.

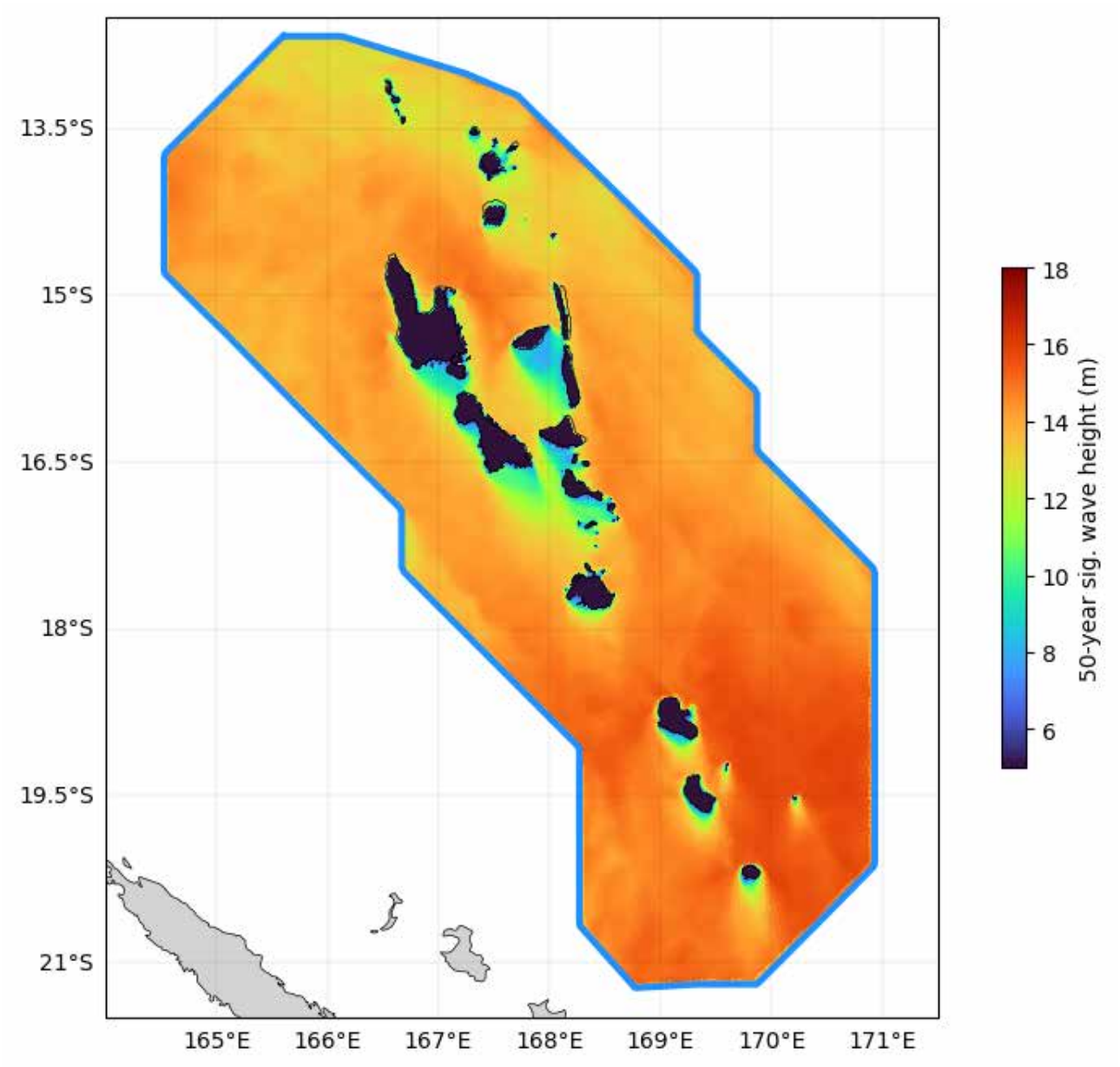

Figure 34: 50-year return period of significant wave height derived from the Ocean Hazard Model probabilistic mode.

5.3 Synthesis of hindcast and probabilistic return periods and inclusion of SLR

Following consultation with VMGD and Van-KIRAP sector leads, the decision was made to provide 10-year, 50-year and 100-year TWL return periods to the Climate Information Services (CIS) underpinning the Vanuatu Climate Futures Portal (https://vanclimatefutures.gov.vu/) for inundation mapping. These are drawn from a combination of the Ocean Hazard Model historic mode and probabilistic mode outputs; these are then convolved with the SLR scenarios described in Section 1.3.1. The methods and rationale for this synthesis is described in the following paragraphs.

The probabilistic mode discussed in the last section greatly reduces the statistical uncertainties in the estimation of TC-related extreme sea level events, particularly at longer return periods. The

probabilistic methods described in sections 4 and 5.2 only consider events when a TC is within the Vanuatu archipelago and are not able to account for extreme water levels that may occur at shorter return periods when no TC is present, for example very high astronomical tides combined with elevated background sea level (sometimes called King tides). This is illustrated in Figure 35, which compares return periods (and statistical uncertainties) derived from the hindcast (historical) and probabilistic modes for an example coastal point. In the example, the historical mode TWLs are higher than probabilistic for return periods between 1 and ~5 years. This is because, statistically speaking, some combination of tide, background sea level and waves not associated with TCs are more likely to produce higher sea levels (TWL) than the likelihood of a TC occurring locally and contributing to the TWL. This pattern of extremes has also been observed in long-term (~100-year) tide gauge records in TC regions (O'Grady et al., 2022). Note also, the statistical uncertainty of the historical mode's return periods is not considerably larger than that of the probabilistic mode at these relatively low return period levels. At return periods >>10 years, however, the historical mode's cone of statistical uncertainties grows rapidly, while the probabilistic mode's uncertainty remains well constrained. Return periods of the wind-wave heights follow similar patterns.

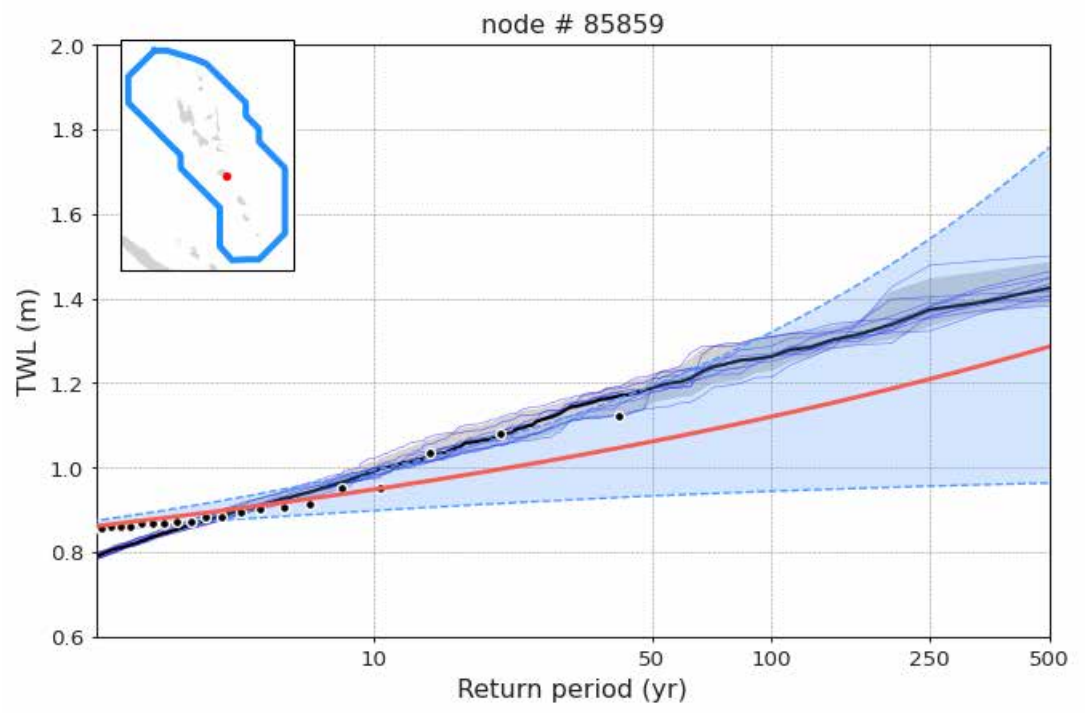

Figure 35: Comparison of Total water level (TWL) return periods derived from the Ocean Hazard Model historic and probabilistic modes for a coastal point on south-east Efate Island. The historically derived empirical return periods, GPD fit and associated uncertainty are indicated by black dots, the red line and blue bands, respectively. The probabilistic (synthetic TC/Monte Carlo emulator TWL derived) are indicated by a black line (median ensemble value) and grey area around the black line and fine blue lines (90% ensemble confidence limits and individual ensemble empirical return periods, respectively).

For these reasons, 10-year return period TWL used to create the inundation mapping within the CIS portal (next section) is drawn from the Ocean Hazard Model historic mode, but the 50- and 100-year return periods are drawn from the Ocean Hazard Model probabilistic mode.

These return periods are then "convolved" with the SLR scenarios developed for Vanuatu (Table 1); for this the median SLR value for each scenario were linearly added to the fitted (for 10-year)

or the ensemble median (for the 50- and 100-year) values; the 5 and 95% uncertainty bands of SLR scenarios were also linearly added to the respective 5 and 95% uncertainty bands of the 10-, 50- and 100-year TWL values. Thus, future sea level scenario coastal extreme sea level return periods contain larger uncertainties than those associated with current (baseline) sea levels. These synthesised return periods are stored as netcdf files with associate metadata. Table 5 gives an indication of these synthesised return periods, when reformatted as a table for several example output points.

Table 5: Example projected TWL return period values for a single coastal point supplied to the CIS portal. This is the same coastal point used for Figure 35. In the column headers, cidix is the index of the point (among the regularly spaced 2331 coastal points); lon, lat is the longitude and latitude of coastal point, respectively; nidx is the nearest "wet" computational node of the numerical model and the water depth of the node. The median values of the 10-, 50- and 100-year return periods of TWL at the coastal point are indicated in the following columns, at each of the future (2030, 2050, 2070 and 2090) time-slices and RCP scenarios. The uncertainty bands for each return period are given in brackets.

	cidx	lon	lat	nidx	depth
	374	168.5415	-17.79935	85859	0.58

year	RCP	10-year		50-year		100-year	
2030	rcp26	1.08	[0.97 - 1.19]	1.32	[1.22 - 1.44]	1.39	[1.30 - 1.51]
	rcp45	1.07	[0.96 - 1.18]	1.31	[1.21 - 1.43]	1.38	[1.29 - 1.50]
	rcp85	1.09	[0.98 - 1.21]	1.32	[1.23 - 1.46]	1.40	[1.30 - 1.54]
2050	rcp26	1.17	[1.05 - 1.39]	1.41	[1.30 - 1.64]	1.49	[1.37 - 1.72]
	rcp45	1.18	[1.05 - 1.42]	1.42	[1.30 - 1.67]	1.50	[1.37 - 1.74]
	rcp85	1.22	[1.06 - 1.51]	1.46	[1.31 - 1.76]	1.54	[1.39 - 1.84]
2070	rcp26	1.27	[1.12 - 1.59]	1.51	[1.37 - 1.84]	1.58	[1.44 - 1.92]
	rcp45	1.31	[1.14 - 1.69]	1.55	[1.39 - 1.94]	1.62	[1.46 - 2.02]
	rcp85	1.42	[1.20 - 1.96]	1.66	[1.45 - 2.21]	1.74	[1.53 - 2.28]
2090	rcp26	1.36	[1.18 - 1.79]	1.60	[1.43 - 2.05]	1.68	[1.50 - 2.12]
	rcp45	1.45	[1.24 - 1.99]	1.69	[1.49 - 2.24]	1.76	[1.57 - 2.32]
	rcp85	1.68	[1.38 - 2.53]	1.92	[1.63 - 2.78]	1.99	[1.70 - 2.85]

5.4 Inundation mapping using the CIS portal

Inundation (marine flood) mapping within the CIS portal utilises the synthesised extreme sea levels (TWL) return periods described in the previous section for all coastal points (for example, see Table 5), in combination with digital elevation models (DEMs) derived from available high-resolution topographic LiDAR data. The return periods for each of the different SLR scenarios are interpolated across the DEM surfaces (using an inverse distance weighting method) to estimate local inundation hazard. Where these inundation hazard layers intersect available coastal asset information (such as roads and buildings), the risk to those assets is estimated. An example of this is shown in Figure 36 and Figure 37: the map interface allows the user to visually inspect the inundation extent of a particular scenario over a recent satellite image; the side bar summarises different information, such as the kilometres of roads inundation under the different SLR scenarios and return periods, in the case of the CIS's Infrastructure section (Figure 37). It should be noted that the median return period values are used for inundation mapping in the CIS, and therefore do

not represent the upper uncertainty bound (worst case scenario) of the TWL return period estimates. This should be considered when interpreting the inundation layer output, along with the additional caveats discussed in the following section.

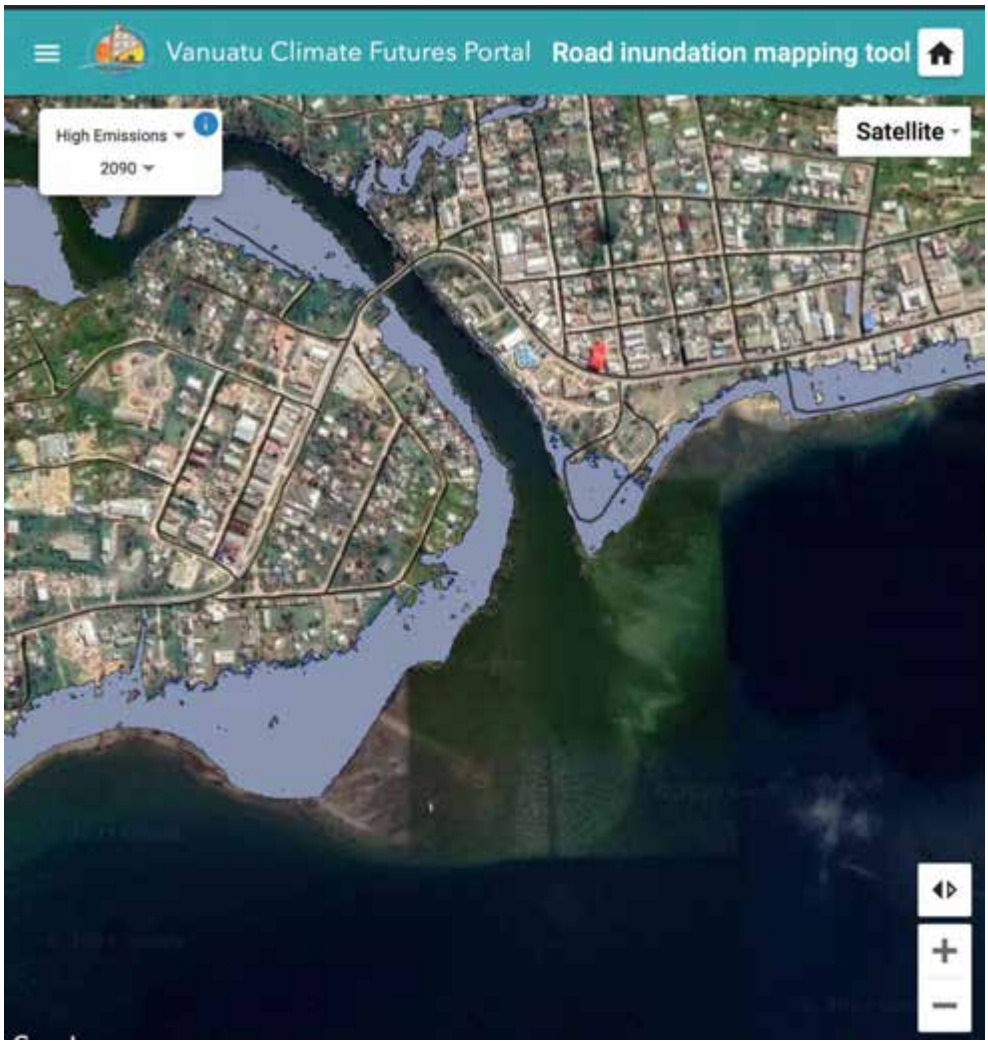

Figure 36: Example inundation layers generated using the Vanuatu Climate Futures Portal

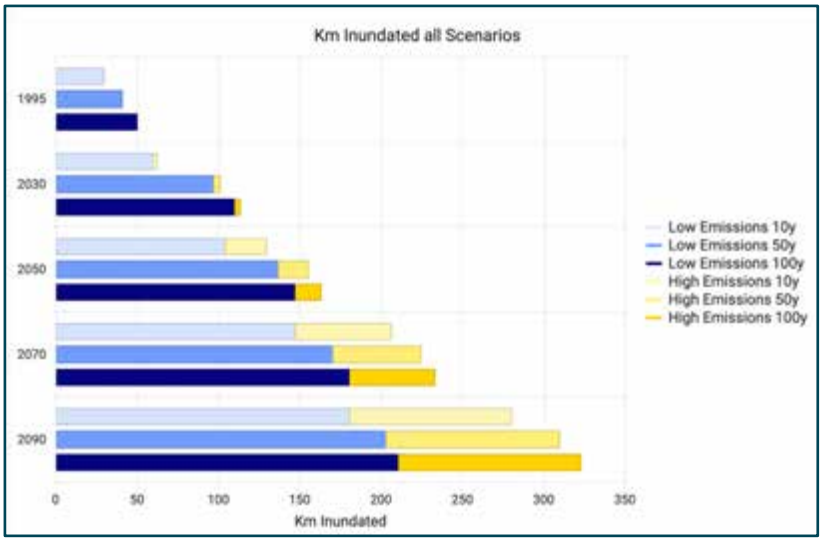

Figure 37: Example inundation-related climate risk information generated using the Vanuatu Climate Futures Portal (https://vanclimatefutures.gov.vu/).

6 Conclusions and recommendations

6.1 Summary and Use Cases

This report provides a technical overview of the Van-KIRAP National Ocean Hazard Modelling System and how it has been utilised in combination with tropical cyclone (TC) modelling (also provided via Van-KIRAP) and sea level rise (SLR) projections to produce extreme value analyses of sea level, storm surge and storm waves capable of informing coastal risk assessments in a nationally consistent fashion. Together with the uploading of key outputs in the form of digitally visualised and spatially referenced CIS products to the Vanuatu Climate Futures Portal (https://vanclimatefutures.gov.vu), this report is the key technical deliverable for Activity 1.2.4 as part of the CSIRO DP scope of work for Van KIRAP.

The underpinning data is delivered via two "modes":

- The hindcast mode, a historical (dynamical) simulation (1980 – 2020) of the combined effects of tides, storm surge, waves and sea level variability.
- The probabilistic mode, consisting of 1000 synthetic TC "scenario" simulations of dynamical storm surge and waves, combined with pre-computed tides, sea level variability and projected SLR in a hybrid/Monte Carlo framework.

The hindcast mode data is best used (for example) as a current climate baseline for coastal waves, water levels and currents, for information on daily or seasonal variance (such as local tides and waves), for historical extreme event attribution and for examining shorter-term (<= 10-year return period) coastal hazards not directly associated with TC events, such as king tides and long-term coastal erosion processes.

The probabilistic mode represents a step forward in the reduction of uncertainties around high impact, low likelihood storm surge and storm wave events and how astronomical tides, sea level variability and future SLR will modulate the associated extreme sea level impacts within Vanuatu.

Following consultation with the Van-KIRAP sectoral stakeholders, 10-, 50- and 100-year return interval extreme sea levels, calculated from extreme value analysis of total water level (TWL) from both modes (as described in previous sections) have been integrated into the on-demand functionality of the Vanuatu Climate Futures Portal; specifically as a tailored CIS product where high-resolution topographic LiDAR survey data are available (currently large areas of Espiritu Santo, Malekula and Efate, see the Van-KIRAP LiDAR factsheet) to allow users to visualize spatially-referenced coastal inundation hazards in coastal areas relevant across multi-decadal (climate change time scales and emissions scenarios. The portal also facilitates calculating associated risk to elements of coastal infrastructure and amenities (e.g. coastal roads and tourist bungalows at the time of writing). As previously alluded however, the underpinning data from the two National Ocean Hazard Modelling System modes can also be used for many other assessments relevant to building climate resilience. For instance, many recent studies have shown the importance of considering the increase in "nuisance flooding" (increases in duration and increased frequency of minor inundation events) with SLR, rather than just considering the severity of rarer extreme

events (see, for example, Moftakhari et al., 2017; Sweet & Park, 2014). The hindcast mode data, alongside the SLR projections is an excellent data set for informing such an assessment in Vanuatu. Conversely, several countries have legislated using extremely long return periods, low likelihood extreme events to be considered when designing flood protection for high value infrastructure assets to attempt to minimise risks associated with otherwise truly catastrophic storms. In this context, and by comparison, United Kingdom and the Netherlands use 1000-year and 10,000-year return period events, respectively (see, for example, Jorissen et al., 2000). Such long return periods can be difficult to establish, but the probabilistic mode presented here provides both the underpinning data and the method to do so for Vanuatu, with some quantification of associated statistical uncertainties involved.

6.2 Caveats

Use of these data for coastal hazard assessments and planning does come with some important technical limitations and caveats. Chief among these:

- This assessment does not include very 'low likelihood high impact' scenarios (i.e. SLR of 1.6 m or greater by 2100) due to poor scientific understanding of Antarctic ice sheet dynamics. Such scenarios are exceedingly unlikely and well outside of the (valid) 5–95 % uncertainty range of the SLR scenarios used in this assessment (Section 1.3.1, Table 1, Figure 3), but they cannot be completely discounted. See van de Wal et al., (2022) for a discussion on such scenarios.
- Depending on application, the National Ocean Hazard Modelling System is unable to adequately resolve nearshore wave breaking and surf-zone processes such as wave setup and runup (see Figure 4 for disambiguation between wave setup and runup) in many areas. This is due to two factors:
    - The finest spatial resolution of the modelling system's computational mesh elements is approximately 250m on a side. While this is a very high resolution for a national modelling system, in many cases it is still insufficient to capture important details of surf-zone processes along Vanuatu's fringing reefs and associated coastlines.
    - The system's component wave model is a spectral, or phase-averaged model. This means that while it does simulate time-averaged wave breaking and subsequent wave setup it does not simulate wave runup. Wave runup and subsequent overtopping of coastal defences (such as seawalls) can locally significantly increase the severity of coastal inundation, particularly along more exposed coastlines. It is also important for estimating erosion hazard.
- This Van-KIRAP activity only considers inundation resulting from ocean processes (e.g. tides, sea level, storm surge and storm waves) and does not include fluvial, pluvial/ocean compound flooding, whereby heavy rain coincides with storm surge (during a TC for instance). This may locally increase inundation severity, particularly in the vicinity of rivers such as the Sarakata and La Colle.

- The more detailed coastal LiDAR datasets (currently only those described in https://www.pacificclimatechange.net/sites/default/files/LiDAR-Vanuatu) used to inform the National Ocean Hazard Modelling System and the Vanuatu Climate Future Portal are not available throughout Vanuatu; in other areas lower spatial resolution and lower accuracy topographic datasets are used. This should be considered when interpreting inundation results and new LiDAR or other high-resolution topographic survey data should be incorporating into analyses when they become available.
- Erosion hazards are not explicitly estimated in this assessment. Hydrodynamic data (waves, tides and currents) provided by the National Ocean Hazard Modelling System can provide insight into coastal erosion, but erosion is a complex process and quantitative hazard estimation requires detailed local geomorphic and geological assessments (Kennedy et al., 2019).

These caveats need to be considered when utilising the model system's outputs and the related Vanuatu Climate Futures Portal's inundation model outputs. These caveats mean that even the upper uncertainty bands and/or higher emissions scenarios of the estimated sea level extremes may still underestimate local inundation hazards in some cases. The recommendations in the next section offer examples of how to ameliorate these underestimations or otherwise how to further increase accuracy/decrease uncertainties in coastal hazard assessment and associated risks for Vanuatu into the future.

6.3 Recommendations for Future Work

The National Ocean Hazard Modelling System, alongside the establishment of an oceanographic monitoring network (Section 3.1.2), both delivered via the Van-KIRAP projects, should be seen as a starting point towards fundamentally improved coastal climate hazard/risk assessment and adaptation planning in Vanuatu. As discussed in previous sections, the system allows for the first nationally consistent extreme sea level (including SLR) and storm wave hazard assessment at the local scale, but limitations of the underpinning data should be considered. Going forward, updates to address these limitations and thereby improve utility of model are recommended in several areas:

- The SLR scenarios used in this study are IPCC AR5-based (CMIP5) and do not include quantification of an upper-limit 'low likelihood high impact' SLR scenario(s). It would be relatively easy to recalculate the projected TWL return periods (like those in Table 5) with updated AR6- and/or other CMIP6-based SLR scenarios when they become available.
- Locations where inundation mapping available within the Vanuatu Climate Futures Portal can be expanded to new areas (or potentially improved in existing areas) as new or improved digital elevation models (DEMs) derived from topographic LiDAR or other high-resolution survey are developed. If improved DEMs cover enough new areas in Vanuatu, it may become worthwhile to perform new hindcast and probabilistic mode simulations, perhaps with modified and/or higher resolution computational mesh topology.
- As outlined in Section 4, the synthetic TC populations used in the probabilistic mode are generated using a historical climate reanalysis. While other studies strongly suggest that SLR has a such a profound effect on (increasing) extreme sea level return periods that the

influence of changes on these return periods due to changes in TC frequency and/or intensity is very minor (e.g. see McInnes et al., 2014), it may be worthwhile to test this using projected future changes to synthetic TC populations to examine if this is the case in Vanuatu.

The above recommendations involve improving or refining the existing coastal hazard modelling system. However, the fidelity and accuracy of local coastal hazard (and risk) assessment can potentially be greatly increased through application of local downscaling models simulating critical aspects of coastal dynamics within the national system. These downscaling models can better account for relevant local processes, thus overcoming many of the caveats outlined in the previous section. For example, several computationally efficient wave runup and empirical/analytical overtopping calculators specifically for reef-lined coasts exist, such as those outlined by (Beetham & Kench, 2018; Merrifield et al., 2014; Scott et al., 2020). There are also dynamical models capable of predicting wave runup and overtopping, such as XBeach (https://github.com/openearth/xbeach), which was employed for a local coastal hazard study for Lanakel, Tanna (Damlamian et al., 2019). Similarly, there are hydrological models capable of simulating compound flooding by simultaneously downscaling ocean forcing (such the waves and water levels provided by the National Ocean Hazard Modelling System and/or the aforementioned wave runup models) and fluvial (stream flow) and pluvial (rain) processes.

Implementing such downscaling models nationally, however, would be complex and computationally expensive, requisite DEMs are not available for large parts of Vanuatu (as previously noted) and requires gathering local input, such as stream gauge observations and geographic/engineering data on flood control structures such as dams and seawalls. Doing this was beyond the remit of the Van-KIRAP project and such site-specific downscaling will likely be performed more on a project-by-project basis, with modelling of restricted geographical extent. For example, an on-going Asian Development Bank (ADB) multi-hazard disaster risk management report used the Van-KIRAP National Ocean Hazard Modelling System to establish both downstream boundary conditions in the fluvial-pluvial inundation assessment and as offshore boundary conditions for coastal inundation for specific extreme sea level event return periods. These offshore boundary conditions were then used to assess the coastal inundation from storm-tide and waves, including infragravity waves using a specialised model used on South Santo area. This illustrates the value of building upon the national system's outputs to provide high-value, high resolution local hazard assessment. It is recommended that similar future projects commit to such local downscaling within a coordinated national framework, allowing the climate vulnerability of coastal assets to be assessed in a nationally consistent and technically robust fashion, building upon previous work including as presented in this report.

7 References

Beetham, E., & Kench, P. S. (2018). Predicting wave overtopping thresholds on coral reef-island shorelines with future sea-level rise. *Nature Communications*, *9*(1), 3997. https://doi.org/10.1038/s41467-018-06550-1

Brown, N. J., Lal, A., Thomas, B., McClusky, S., Dawson, J., Hu, G., & Jia, M. (2020). *Vertical motion of Pacific Island tide gauges: combined analysis of GNSS and levelling*. Geoscience Australia. https://doi.org/10.11636/record.2020.003

Camus, P., Cofiño, A. S., Mendez, F. J., & Medina, R. (2011). Multivariate wave climate using self-organizing maps. *Journal of Atmospheric and Oceanic Technology*. https://doi.org/10.1175/JTECH-D-11-00027.1

Chen, W.-B., Chen, H., Hsiao, S.-C., Chang, C.-H., & Lin, L.-Y. (2019). *Wind forcing effect on hindcasting of typhoon-driven extreme waves*. https://doi.org/10.1016/j.oceaneng.2019.106260

Coles, S. (2001). *An Introduction to Statistical Modeling of Extreme Values*. Springer London. https://doi.org/10.1007/978-1-4471-3675-0

CSIRO, & SPREP. (2021). *Current and future climate for Vanuatu: enhanced "NextGen" projections Technical report*. https://doi.org/10.25919/hexz-1r10

Damlamian, H., Bosserelle, C., Raj, A., Begg, Z., Katterborn, T., Ketewai, M., Kruger, J., Naki, N., & Jean Claude Willie, M. S. (2017). *Tropical Cyclone Pam: A report on the coastal inundation assessment undertaken in Vanuatu using an unmanned aerial vehicle (UAV)*.

Damlamian, H., Wandres, M., Giblin, J., Jackson, N., Begg, Z., Degei, P., Kumar, S., Kruger, J., Kanas, T., Aru, R., & Naki, N. (2019). *Probabilitic cyclone and swell-driven inundation hazard assessment, Lenakel, Tanna, Vanuatu*.

Durrant, T., Greenslade, D., Hemar, M., & Trenham, C. (2014). A Global Hindcast focussed on the Central and South Pacific. *CAWCR Technical Report*.

Egbert, G. D., Erofeeva, S. Y., Egbert, G. D., & Erofeeva, S. Y. (2002). Efficient Inverse Modeling of Barotropic Ocean Tides. *Journal of Atmospheric and Oceanic Technology*, *19*(2), 183–204. https://doi.org/10.1175/1520-0426(2002)019<0183:EIMOBO>2.0.CO;2

Emanuel, K., Ravela, S., Vivant, E., & Risi, C. (2006). A statistical deterministic approach to hurricane risk assessment. *Bulletin of the American Meteorological Society*, *87*(3), 299–314. https://doi.org/10.1175/BAMS-87-3-299

Emanuel, K., Sundararajan, R., & Williams, J. (2008). Hurricanes and Global Warming: Results from Downscaling IPCC AR4 Simulations. *Bulletin of the American Meteorological Society*, *89*(3), 347–368. https://doi.org/10.1175/BAMS-89-3-347

Fasullo, J. T., & Nerem, R. S. (2018). Altimeter-era emergence of the patterns of forced sea-level rise in climate models and implications for the future. *Proceedings of the National Academy of Sciences*, *115*(51), 12944–12949. https://doi.org/10.1073/pnas.1813233115

Fleming, J. G., Fulcher, C. W., Luettich, R. A., Estrade, B. D., Allen, G. D., & Winer, H. S. (2008). A Real Time Storm Surge Forecasting System Using ADCIRC. *Proceedings of the International Conference on Estuarine and Coastal Modeling*, 893–912. https://doi.org/10.1061/40990(324)48

Hoeke, R. K., Damlamian, H., Aucan, J., & Wandres, M. (2021). Severe Flooding in the Atoll Nations of Tuvalu and Kiribati Triggered by a Distant Tropical Cyclone Pam. *Frontiers in Marine Science*, *7*, 991. https://doi.org/10.3389/fmars.2020.539646

Hoeke, R. K., Mcinnes, K. L., Kruger, J. C., Mcnaught, R. J., Hunter, J. R., & Smithers, S. G. (2013). Widespread inundation of Pacific islands triggered by distant-source wind-waves. *Global and Planetary Change*, *108*, 128–138. https://doi.org/10.1016/j.gloplacha.2013.06.006

Holland, G. J., Belanger, J. I., & Fritz, A. (2010). A Revised Model for Radial Profiles of Hurricane Winds. *Monthly Weather Review*, *138*(12), 4393–4401. https://doi.org/10.1175/2010MWR3317.1

Iwamoto, M. M., Langenberger, F., & Ostrander, C. E. (2016). Ocean observing: Serving stakeholders in the Pacific Islands. *Marine Technology Society Journal*, *50*(3), 47–54. https://doi.org/10.4031/MTSJ.50.3.2

Jorissen, R., Litjens, J., & Mendez Lorenzo, A. (2000). *Flooding risk in coastal areas. Risks, safety levels and probabilistic techniques in five countries along the North Sea coast*.

Kennedy, A. B., Westerink, J. J., Smith, J. M., Hope, M. E., Hartman, M., Taflanidis, A. A., Tanaka, S., Westerink, H., Cheung, K. F., Smith, T., Hamann, M., Minamide, M., Ota, A., & Dawson, C. (2012). Tropical cyclone inundation potential on the Hawaiian Islands of Oahu and Kauai. *Ocean Modelling*, *52–53*, 54–68. https://doi.org/10.1016/j.ocemod.2012.04.009

Kennedy, D. M., McInnes, K., & Ierodiaconou, D. (2019). *Understanding coastal erosion on beaches: A guide for managers, policy makers and citizen scientists*.

Kirono, D., Round, V., Ramsay, H., Thatcher, M., Nguyen, K., Rafter, T., & Takbash, A. (2023). *National and sub-national climate projections for Vanuatu*.

Knapp, K. R., Kruk, M. C., Levinson, D. H., Diamond, H. J., Neumann, C. J., Knapp, K. R., Kruk, M. C., Levinson, D. H., Diamond, H. J., & Neumann, C. J. (2010). The International Best Track Archive for Climate Stewardship (IBTrACS). *Bulletin of the American Meteorological Society*, *91*(3), 363–376. https://doi.org/10.1175/2009BAMS2755.1

Lin, N., Emanuel, K. A., Smith, J. A., & Vanmarcke, E. (2010). Risk assessment of hurricane storm surge for New York City. *Journal of Geophysical Research: Atmospheres*, *115*(D18), 18121. https://doi.org/10.1029/2009JD013630

Madsen, O., Poon, Y., & Graber, H. (1988). Spectral Wave Attenuation by Bottom Friction: Theory. *Coastal Engineering*, *1*(21). http://journals.tdl.org/icce/index.php/icce/article/viewArticle/4241

Marra, J. J., Gooley, G., Johnson, M.-V. V., Keener, V. W., Kruk, M. K., Potemra, J. T., & Warrick, O. (2022). *Pacific Climate Change Monitor: 2021*. The Pacific Islands-Regional Climate Centre (PI-RCC) Network Report to the Pacific Islands Climate Service (PICS) Panel and Pacific Meteorological Council. https://doi.org/10.5281/zenodo.6965143

Mcinnes, K. L., Grady, J. G. O., Walsh, K. J. E., & Colberg, F. (2011). *Progress Towards Quantifying Storm Surge Risk in Fiji due to Climate Variability and Change*. *64*, 1121–1124.

McInnes, K. L., Walsh, K. J. E., Hoeke, R. K., O'Grady, J. G., Colberg, F., & Hubbert, G. D. (2014). Quantifying storm tide risk in Fiji due to climate variability and change. *Global and Planetary Change*, *116*, 115–129. https://doi.org/10.1016/j.gloplacha.2014.02.004

Merrifield, M. A., Becker, J. M., Ford, M., & Yao, Y. (2014). Observations and estimates of wave-driven water level extremes at the Marshall Islands. *Geophysical Research Letters*, *41*(20), 7245–7253. https://doi.org/10.1002/2014GL061005

Moftakhari, H. R., AghaKouchak, A., Sanders, B. F., & Matthew, R. A. (2017). Cumulative hazard: The case of nuisance flooding. *Earth's Future*, *5*(2), 214–223. https://doi.org/10.1002/2016EF000494

Nicholls, R. J., Wong, P. P., Burkett, V. R., Codignotto, J., Hay, J. E., McLean, R. F., Ragoonaden, S., & Woodroffe, C. D. (2007). Coastal systems and low-lying areas. Climate change 2007: Impacts, adaptation and vulnerability. In *Coastal Systems and Low-lying Areas In: Climate Change 2007: Impacts, Adaptation and Vulnerability*. http://www.scopus.com/inward/record.url?eid=2-s2.0-83155174880&partnerID=tZOtx3y1

O'Grady, J. G., Stephenson, A. G., & McInnes, K. L. (2022). Gauging mixed climate extreme value distributions in tropical cyclone regions. *Scientific Reports 2022 12:1*, *12*(1), 1–9. https://doi.org/10.1038/s41598-022-08382-y

Powell, M. D., Vickery, P. J., & Reinhold, T. A. (2003). Reduced drag coefficient for high wind speeds in tropical cyclones. *Nature 2003 422:6929*, *422*(6929), 279–283. https://doi.org/10.1038/nature01481

Ribal, A., & Young, I. R. (2019). 33 years of globally calibrated wave height and wind speed data based on altimeter observations. *Scientific Data*, *6*(1), 77. https://doi.org/10.1038/s41597-019-0083-9

Scott, F., Antolinez, J. A. A., McCall, R., Storlazzi, C., Reniers, A., & Pearson, S. (2020). Hydro-Morphological Characterization of Coral Reefs for Wave Runup Prediction. *Frontiers in Marine Science*, *7*, 531672. https://doi.org/10.3389/FMARS.2020.00361/BIBTEX

Seneviratne, S. I., Nicholls, N., Easterling, D., Goodess, C. M., Kanae, S., Kossin, J., Luo, Y., Marengo, J., McInnes, K., Rahimi, M., Reichstein, M., Sorteberg, A., Vera, C., & Zhang, X. (2012). Changes in climate extremes and their impacts on the natural physical environment: An overview of the IPCC SREX report. *EGU General Assembly 2012*. http://adsabs.harvard.edu/abs/2012EGUGA..1412566S

Smith, G. A., Hemer, M., Greenslade, D., Trenham, C., Zieger, S., & Durrant, T. (2020). Global wave hindcast with Australian and Pacific Island Focus: From past to present. *Geoscience Data Journal*, gdj3.104. https://doi.org/10.1002/gdj3.104

Sweet, W. V., & Park, J. (2014). From the extreme to the mean: Acceleration and tipping points of coastal inundation from sea level rise. *Earth's Future*, *2*(12), 579–600. https://doi.org/10.1002/2014EF000272

The World Bank Group. (2021). *Climate Risk Country Profile: Vanuatu* .

van de Wal, R. S. W., Nicholls, R. J., Behar, D., McInnes, K., Stammer, D., Lowe, J. A., Church, J. A., DeConto, R., Fettweis, X., Goelzer, H., Haasnoot, M., Haigh, I. D., Hinkel, J., Horton, B. P., James, T. S., Jenkins, A., LeCozannet, G., Levermann, A., Lipscomb, W. H., … White, K. (2022). A High-End Estimate of Sea Level Rise for Practitioners. *Earth's Future*, *10*(11), e2022EF002751. https://doi.org/10.1029/2022EF002751

van Vloten, S. O., Cagigal, L., Pérez-Díaz, B., Hoeke, R., & Méndez, F. J. (2024). SHyTCWaves: A stop-motion hybrid model to predict tropical cyclone induced waves. *Ocean Modelling*, *188*, 102341. https://doi.org/10.1016/J.OCEMOD.2024.102341

van Vloten, S. O., Cagigal, L., Rueda, A., Ripoll, N., & Méndez, F. J. (2022). HyTCWaves: A Hybrid model for downscaling Tropical Cyclone induced extreme Waves climate. *Ocean Modelling*, *178*, 102100. https://doi.org/10.1016/J.OCEMOD.2022.102100

Wandres, M., Aucan, J., Espejo, A., Jackson, N., De Ramon N'Yeurt, A., & Damlamian, H. (2020). Distant-Source Swells Cause Coastal Inundation on Fiji's Coral Coast. *Frontiers in Marine Science*, *7*. https://doi.org/10.3389/fmars.2020.00546

Zhang, Y. J., Ye, F., Stanev, E. V, & Grashorn, S. (2016). Seamless cross-scale modeling with SCHISM. *Ocean Modelling*, *102*, 64–81. https://doi.org/10.1016/j.ocemod.2016.05.002


KLAEMET
SAVE
REDI · ADAPT · PROTEKT


LONG GOD YUMI STRONG

Department Vanuatu Meteorology and Geo-Hazards

CSIRO

SPREP
Secretariat of the Pacific Regional
Environment Programme

GREEN
CLIMATE
FUND